Measurement of cross sections and properties of the Higgs boson in decays to bosons using the ATLAS detector

Lucrezia Stella Bruni
on behalf of the ATLAS collaboration

CIPANP 2018
29/05/2018

Higgs boson decay to di-bosons

Bosonic decay channels present quite low branching fractions, but have a **clean signature** and are a powerful tool for many Higgs boson **properties** measurements

$H \to \gamma\gamma$

BR~0.2%

S/B~0.03

- Good mass resolution
- Moderate sample size

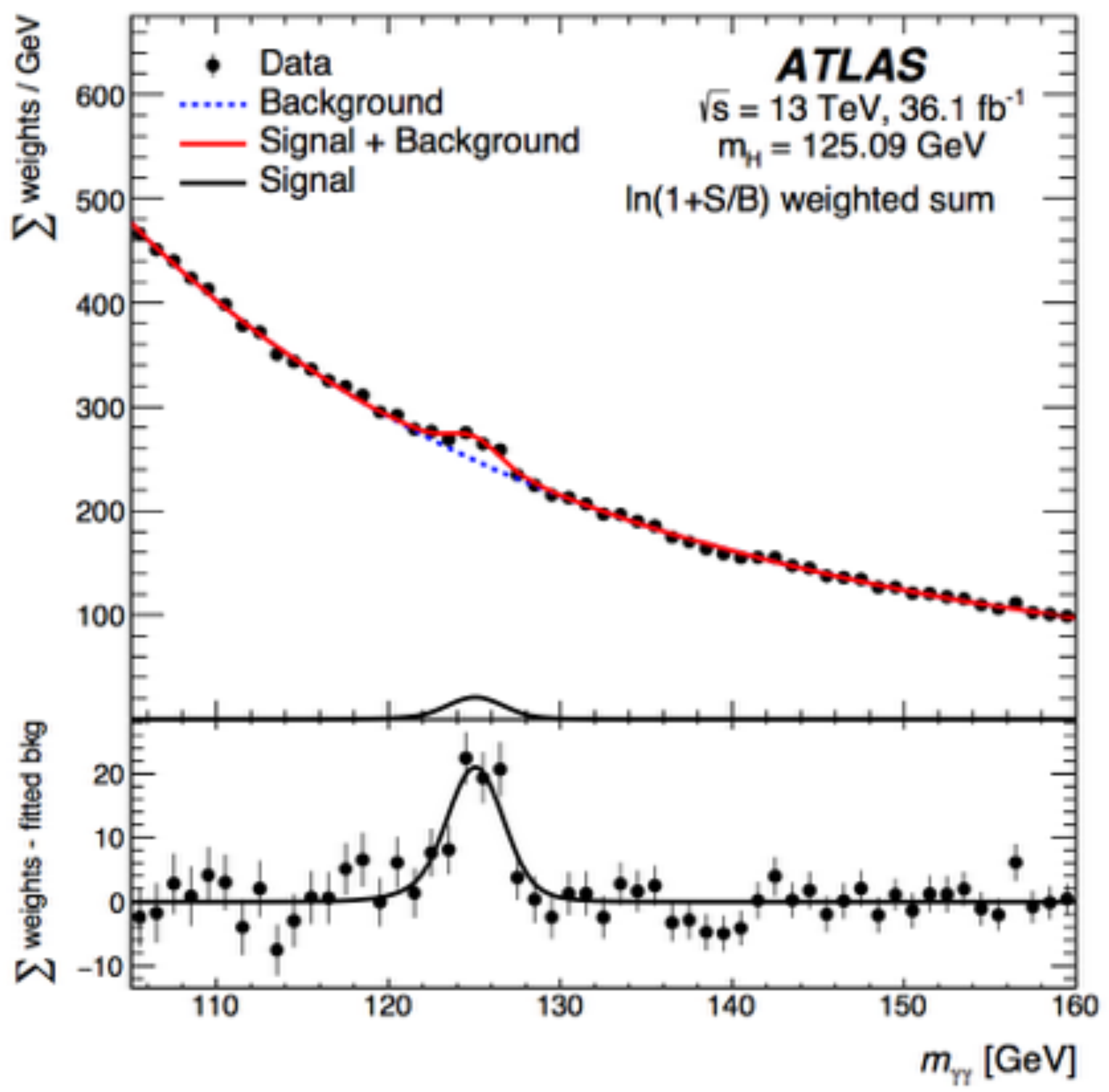

$H \to ZZ^* \to 4l$

BR ~0.013%, l=e,μ

S/B~2.3

- Good mass resolution
- Best S/B ratio
- Limited stats

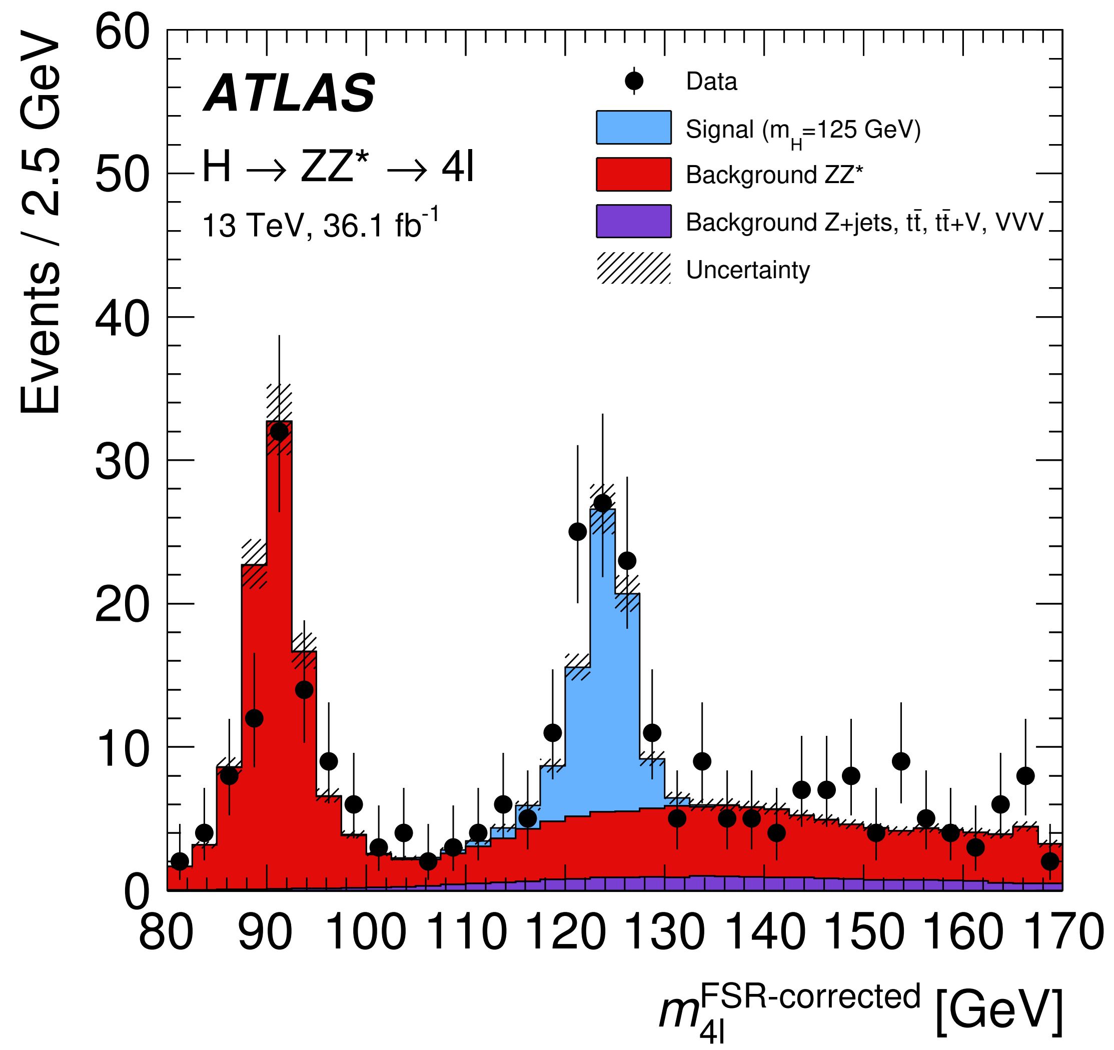

$H \to WW^* \to l\nu l\nu$

BR ~1.5%, l=e,μ, $\tau \to l\nu\nu$

S/B~0.14

- Good branching fraction
- Poor mass resolution
- Large backgrounds

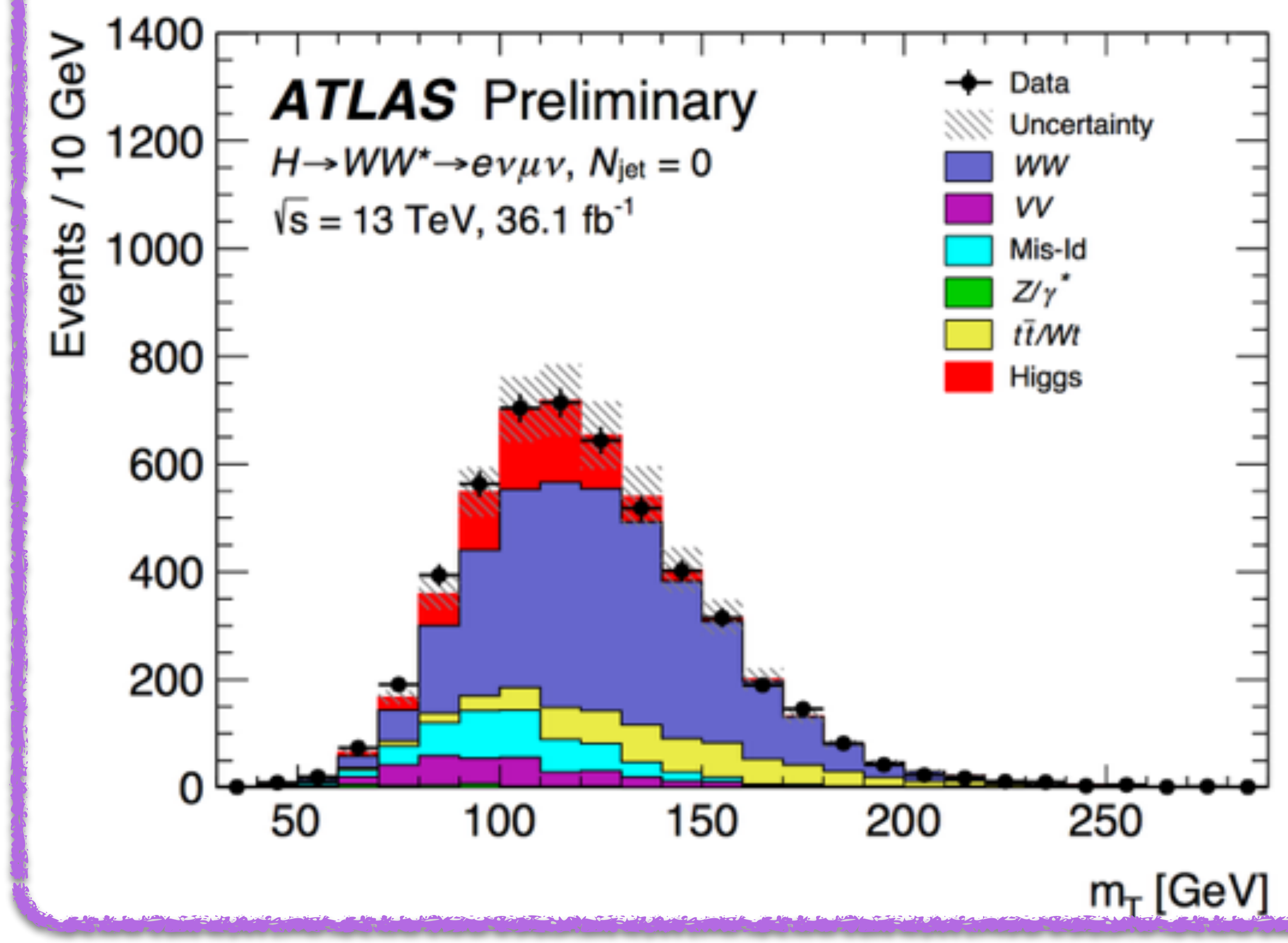

Higgs boson decay to di-bosons

Bosonic decay channels present quite low branching fractions, but have a **clean signature** and are a powerful tool for many Higgs boson **properties** measurements

H→$\gamma\gamma$

BR~0.2%

S/B~0.03

- Good mass res
- Moderate sam

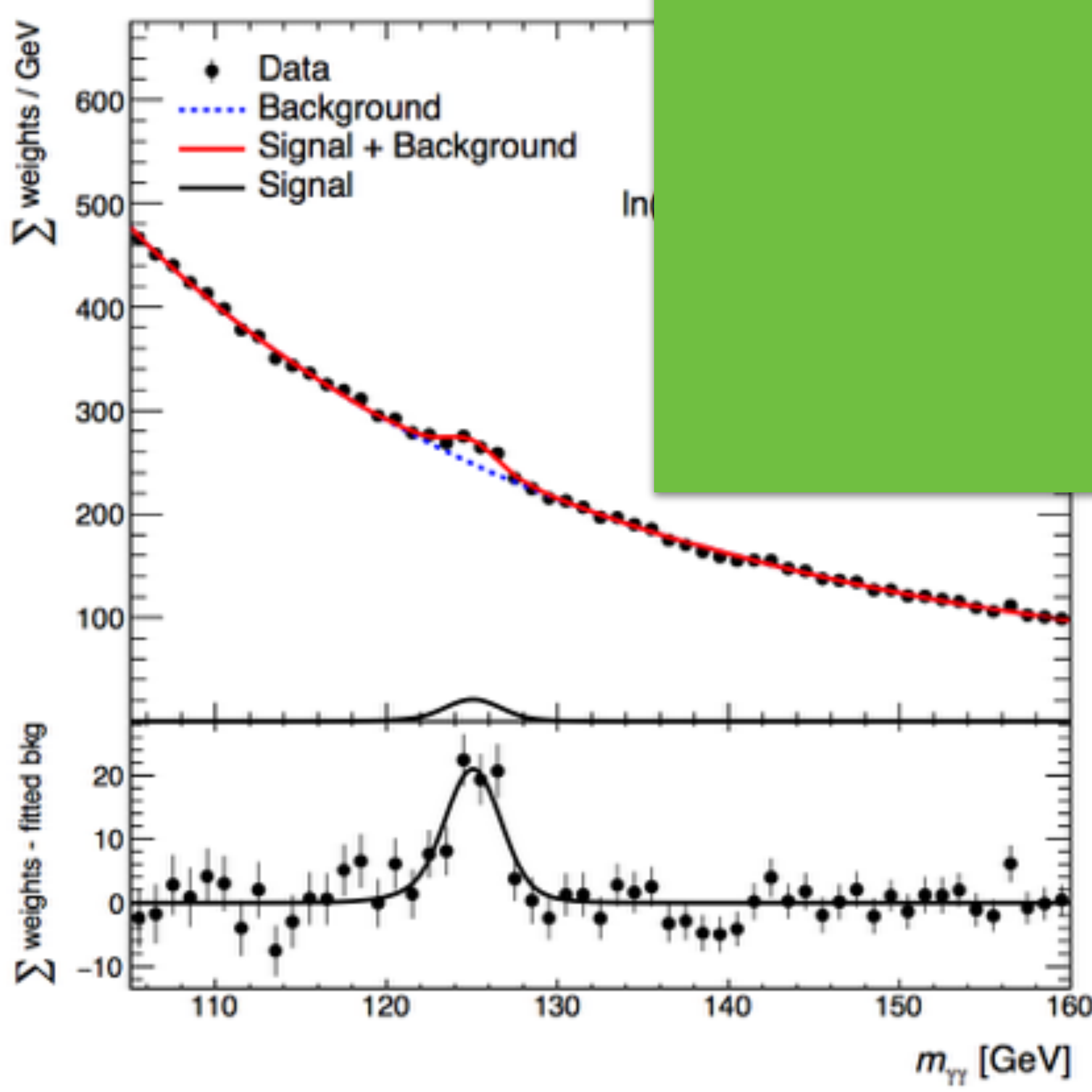

H→ZZ*→4l

BR ~0.013%, l=e,μ

S/B~2.3

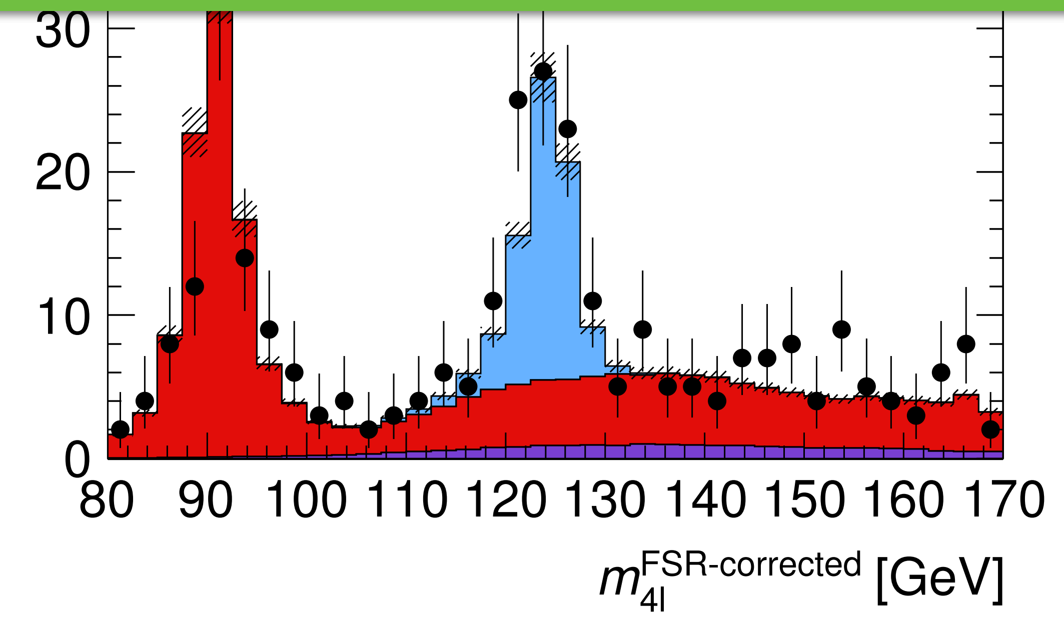

H→WW*→lνlν

BR ~1.5%, l=e,μ, τ→lνν

S/B~0.14

hing fraction

esolution

rounds

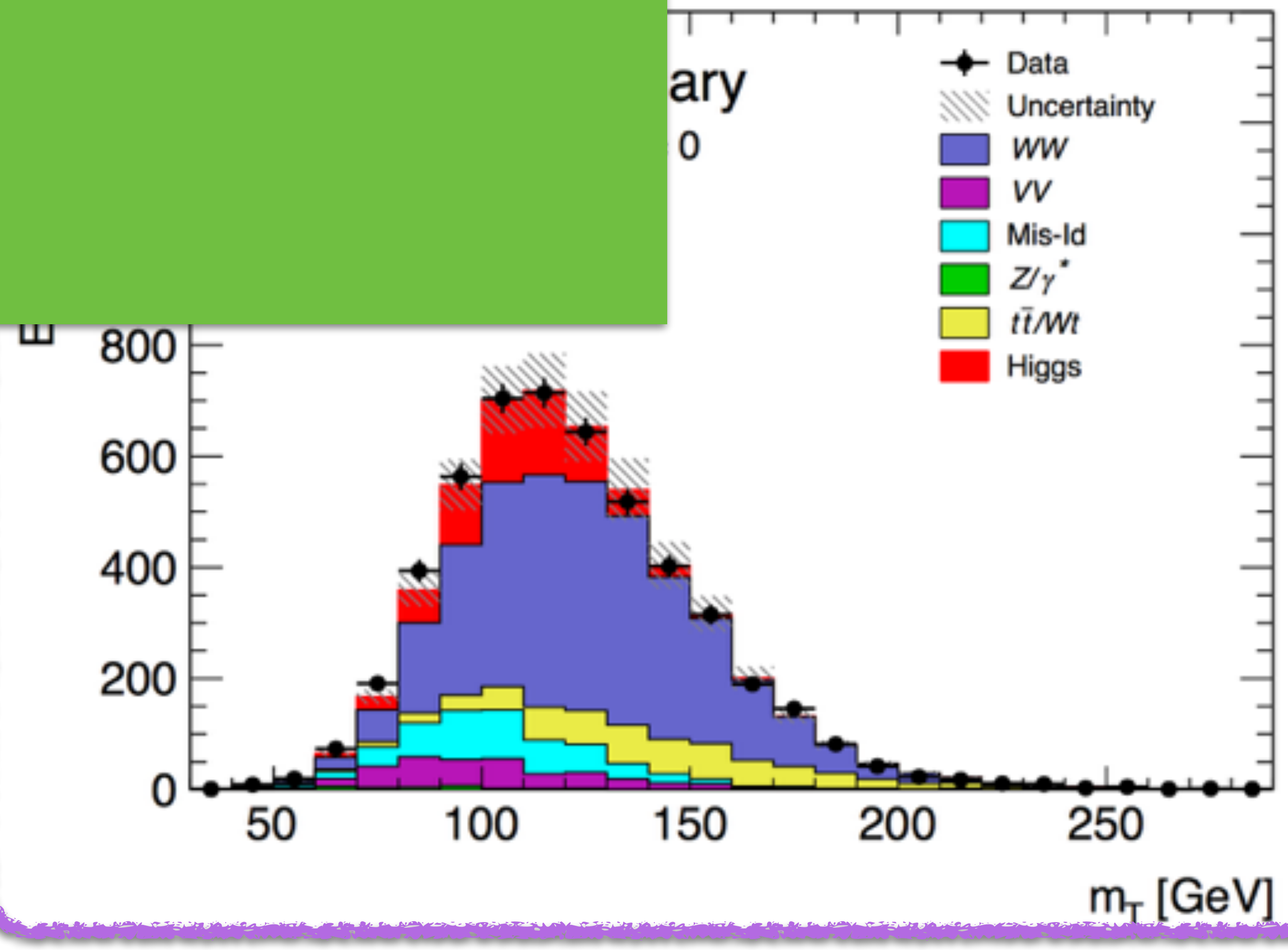

All analyses in this talk are with Run 2 2015+2016 data 36.1 fb^{-1}

Cross section measurements

In Run-2 different Higgs boson cross-section measurements considered:

Production cross-section: usually expressed as signal strength $\mu = \frac{\sigma \times \mathrm{B}}{(\sigma \times \mathrm{B})_{\mathrm{SM}}}$

Simplified template cross-section (STXS)

Exclusive regions of phase space ("bins") specific to the different production modes.

- Different stages with increasing number of production bins
- Minimise the dependence on theoretical uncertainties
- Ease combination of decay channels

Fiducial inclusive and differential cross-section:

$$\sigma_{i,\mathrm{fid}} = \sigma_i \times A_i \times \mathcal{B} = \frac{N_{i,\mathrm{fit}}}{\mathcal{L} \times C_i}, \quad C_i = \frac{N_{i,\mathrm{reco}}}{N_{i,\mathrm{part}}}$$

Fiducial: measured in a fiducial volume:

No acceptance correction → **Measurements largely model-independent**

Allows to introduce the theory uncertainty in a second interpretation step

The resulting **inclusive** cross sections and **differential distributions** (as $p_{\mathrm{T}}^{\mathrm{H}}$, $|y^{\mathrm{H}}|$) can be used to test the expected SM properties of the Higgs boson and its production

Model independence

Higgs boson mass measurement

Higgs boson mass measured in H→ZZ*→4ℓ/H→γγ channels

Channels with fully reconstructed narrow peak over a smooth background

Statistically limited channel

Limited by photon energy scale systematic uncertainties

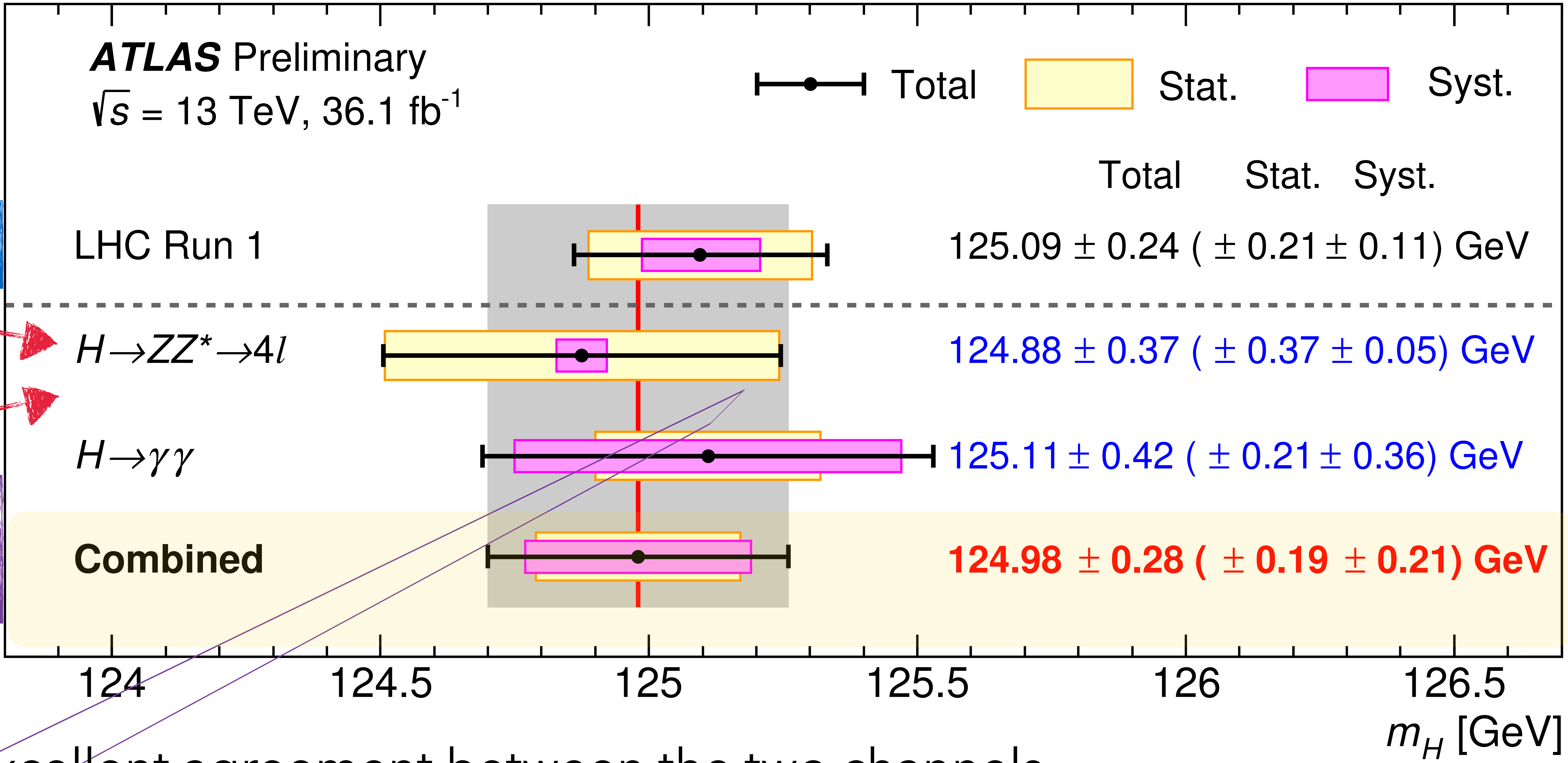

Excellent agreement between the two channels

$$\Delta m_H = 0.23 \pm 0.42\ (\text{stat}) \pm 0.36\ (\text{syst})\ \text{GeV} = 0.23 \pm 0.55\ \text{GeV}.$$

H→WW*→eνμν analysis

ATLAS-CONF-2018-004 Newest results!

Signal: two prompt opposite sign and flavour isolated leptons with small opening angle and missing transverse energy

Backgrounds:

- WW, tt,tW, Z/γ∗ → ττ : constrained with data control regions
- Mis-identified leptons in W + jets and multijets events: fake factor methods from Z + jets data
- Other diboson (WZ, ZZ, Wγ) from MC

Analysis strategy

- Events classified in three Signal Regions (Njets):

  - Njets = 0 , Njets = 1

    gluon-gluon fusion (ggF):

    m_T used as discriminant

$$m_T = \sqrt{\left(E_T^{\ell\ell} + E_T^{miss}\right)^2 - \left|\mathbf{p}_T^{\ell\ell} + \boldsymbol{E}_T^{\rm miss}\right|^2}$$

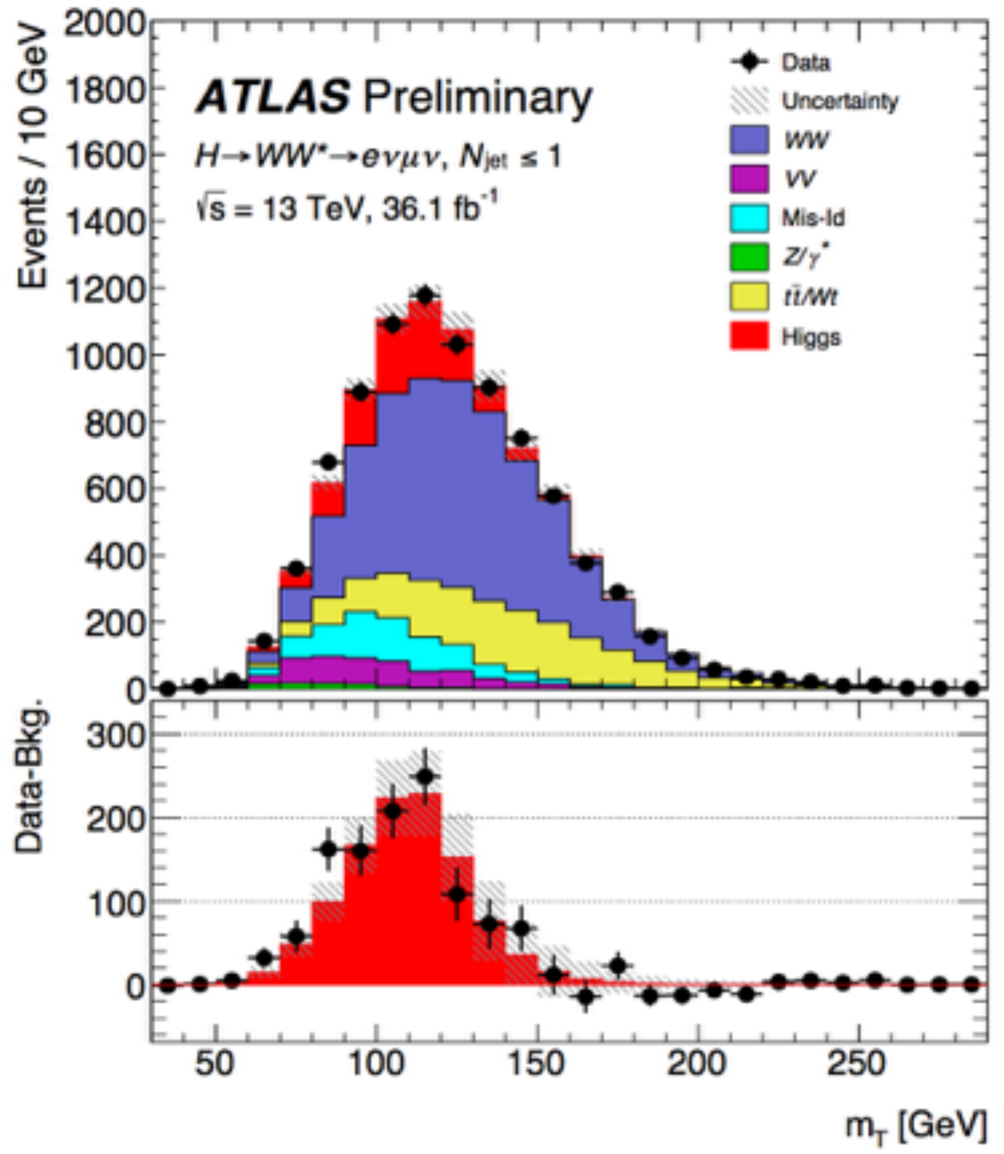

  - Njets ≥ 2

    Vector Boson Fusion (VBF)

    BDT used as discriminant

    built from jet/lepton kin. quantities

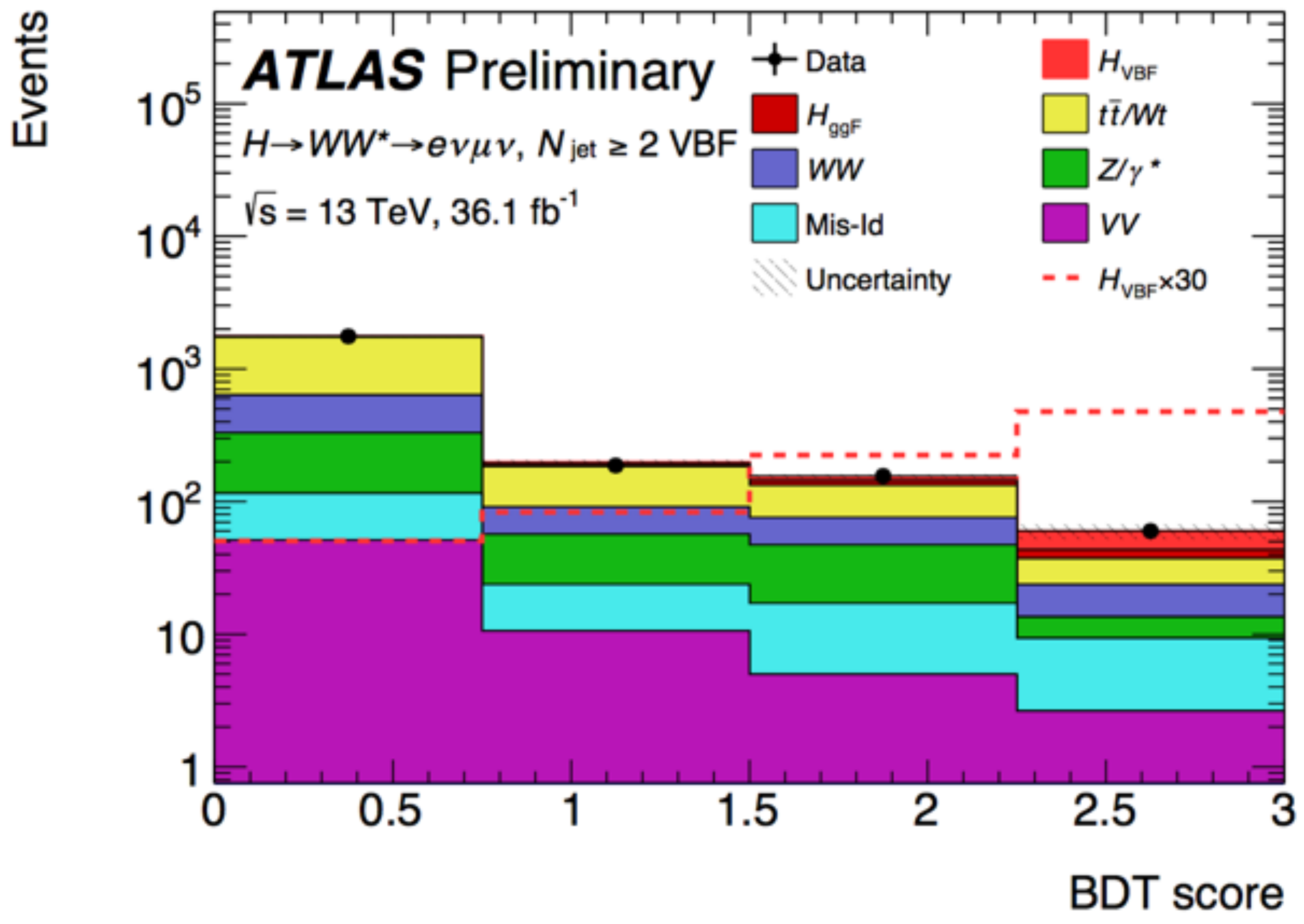

H→WW*→eνμν - Production cross-section

Performed combined maximum likelihood fits of the SR /CR

Significance

ggF: 6.3σ (exp.5.2σ)
VBF: 1.9σ (exp.2.7σ)

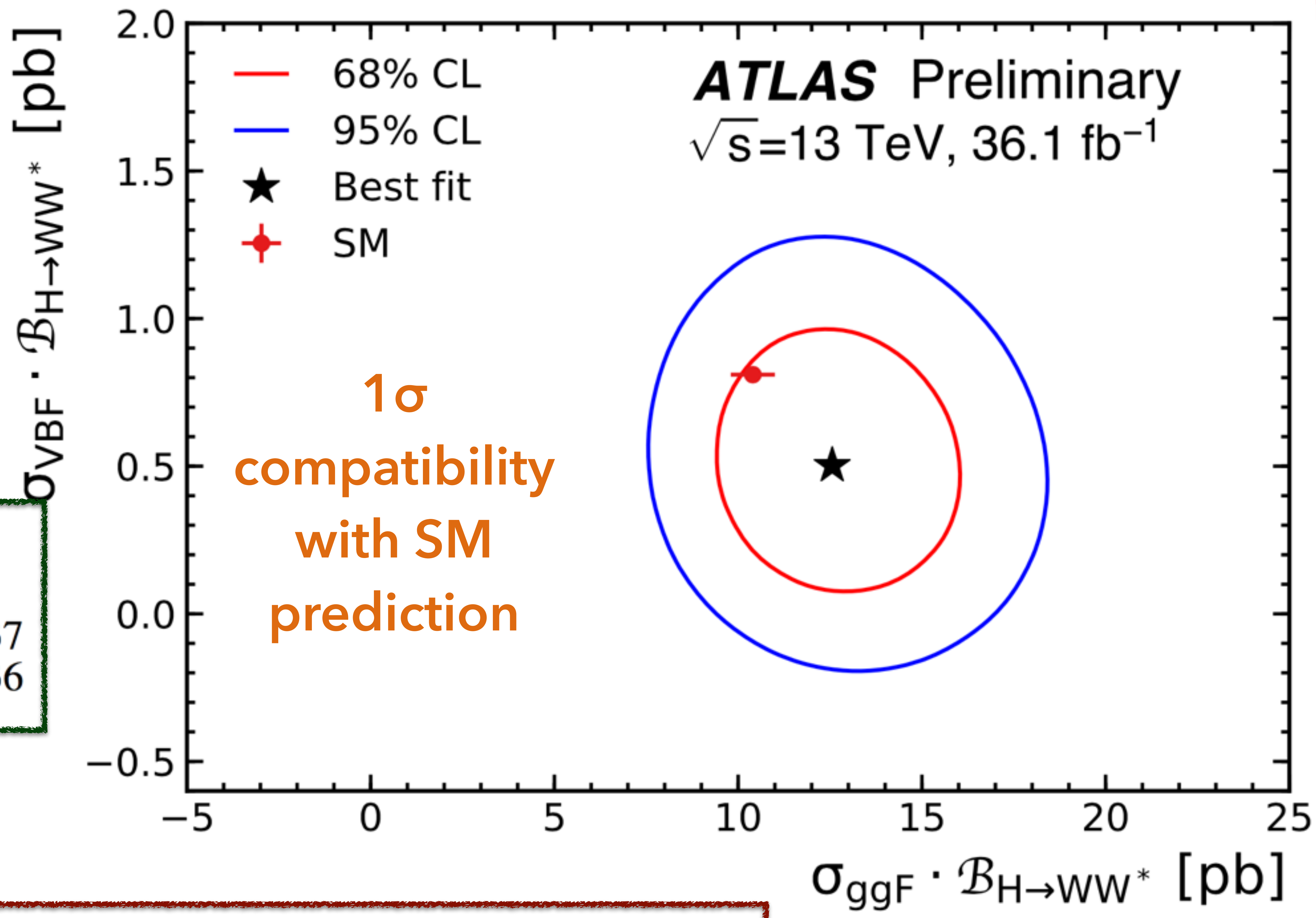

Signal strengths:

$$\mu_{\text{ggF}} = 1.21^{+0.12}_{-0.11}(\text{stat.})^{+0.18}_{-0.17}(\text{sys.}) = 1.21^{+0.22}_{-0.21}$$
$$\mu_{\text{VBF}} = 0.62^{+0.30}_{-0.28}(\text{stat.}) \pm 0.22(\text{sys.}) = 0.62^{+0.37}_{-0.36}$$

Cross section results:

$$\sigma_{\text{ggF}} \cdot \mathcal{B}_{H\to WW^*} = 12.6^{+1.3}_{-1.2}(\text{stat.})^{+1.9}_{-1.8}(\text{sys.})\text{ pb} = 12.6^{+2.3}_{-2.1}\text{ pb}$$
$$\sigma_{\text{VBF}} \cdot \mathcal{B}_{H\to WW^*} = 0.50^{+0.24}_{-0.23}(\text{stat.}) \pm 0.18(\text{sys.})\text{ pb} = 0.50^{+0.30}_{-0.29}\text{ pb}$$

Predicted σ_{ggF}×BR=10.4±0.6 pb and σ_{VBF}×BR=0.81±0.02

H→γγ -Production cross section

arXiv:1802.04146v1

Signal yield extracted from simultaneous signal+bkg fit of mγγ distribution

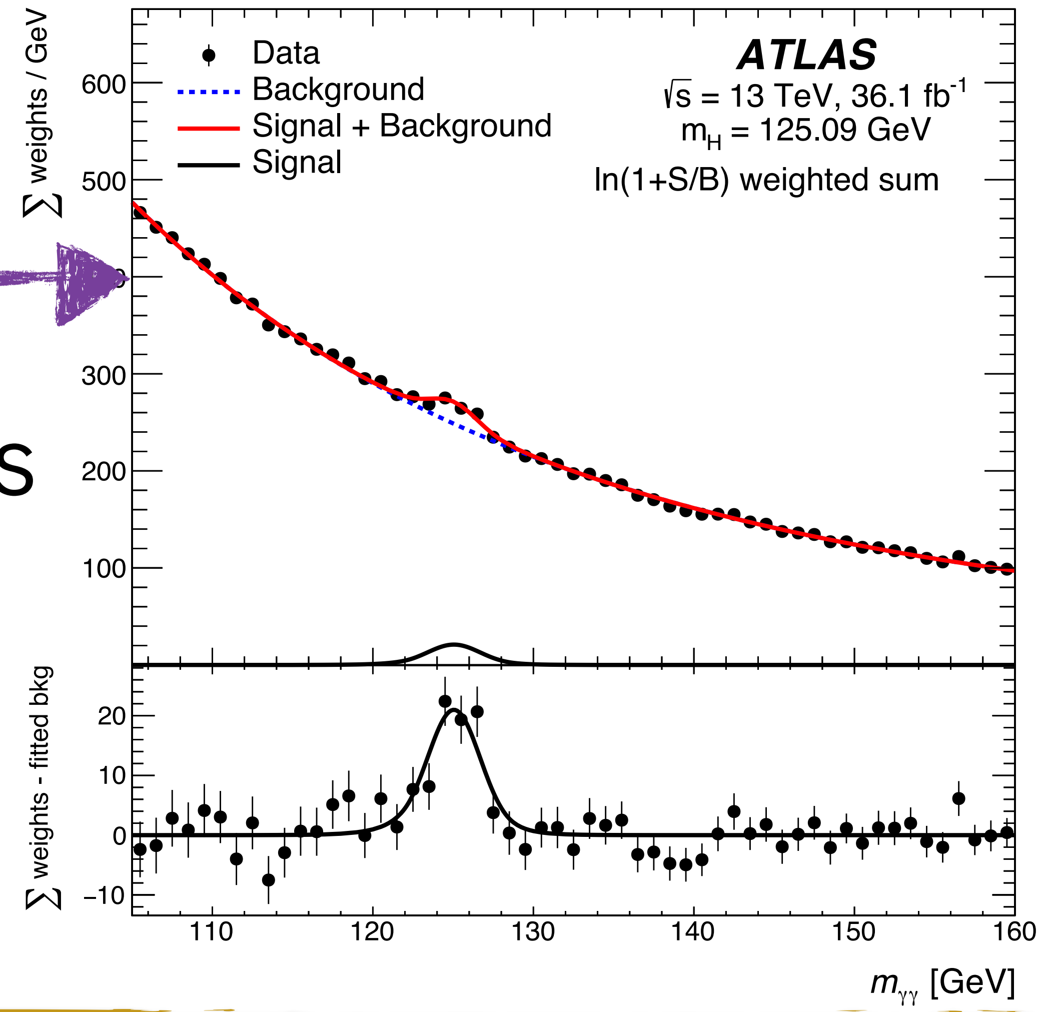

Analysis performed with event categorisations that targets H production modes

Production mode cross-section x BR

- Simplified Template Cross-Sections (STXS)
- Exclusive regions, reducing theory dependence while maximising experimental sensitivity

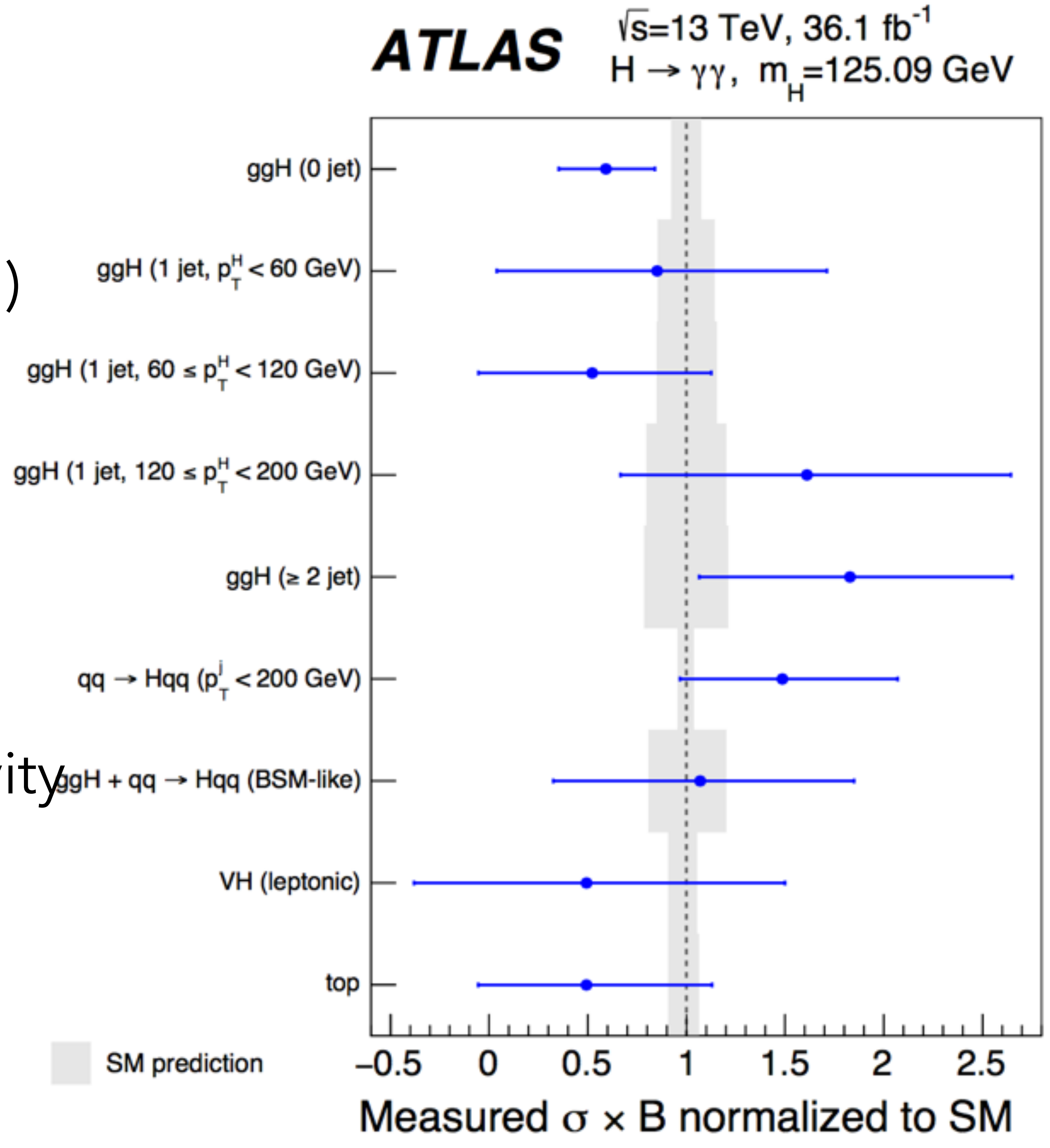

Signal strength

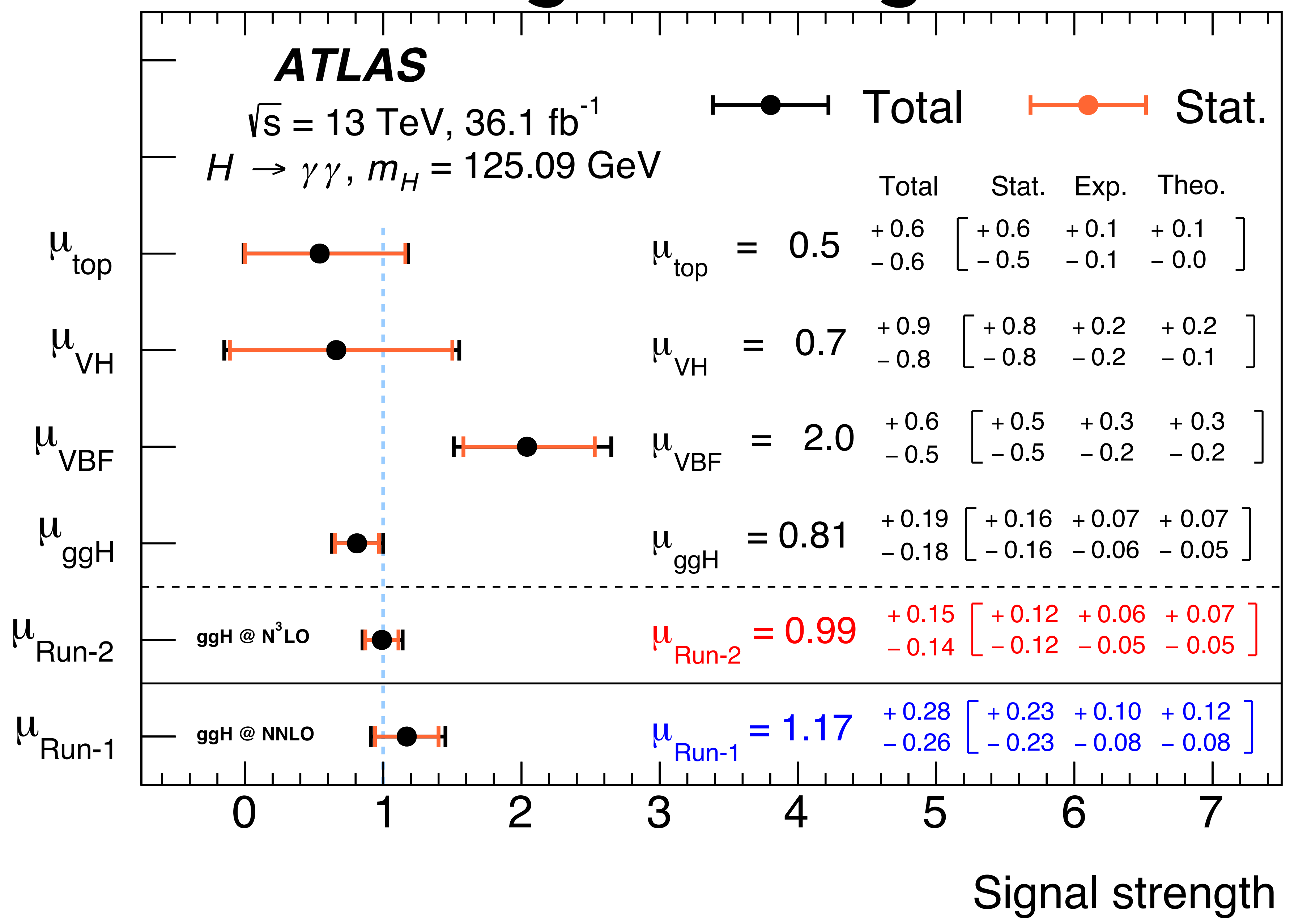

Good agreement with SM predictions

arXiv:1802.04146v1

H→γγ - Fiducial cross section

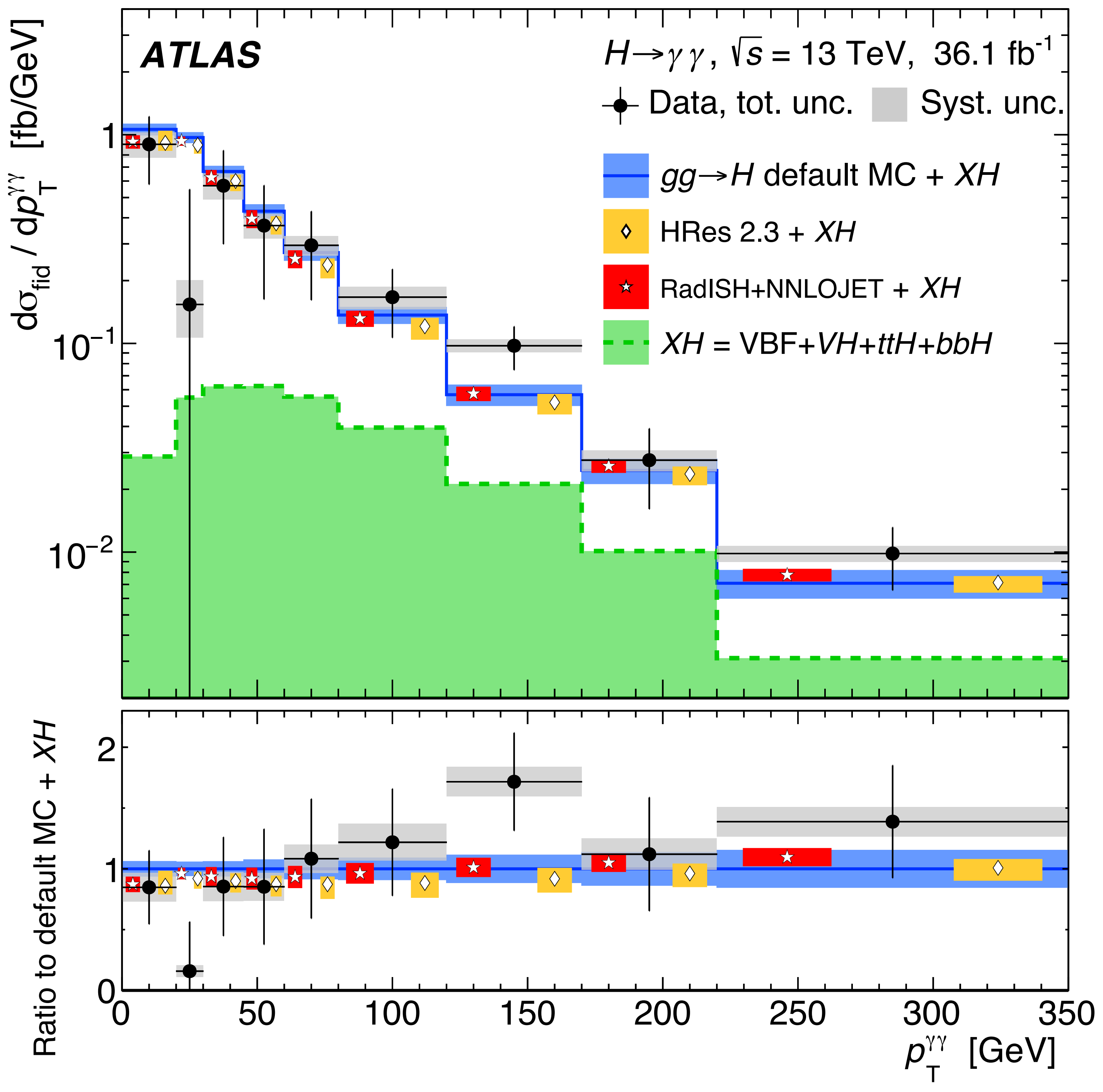

- The H → γγ signal is extracted using a fit to the mγγ distribution
- Signal yields corrected for experimental inefficiencies and resolution effects
  1) Inclusive in production mode
  2) Separately in fiducial phase space enhancing the contribution of the different production modes

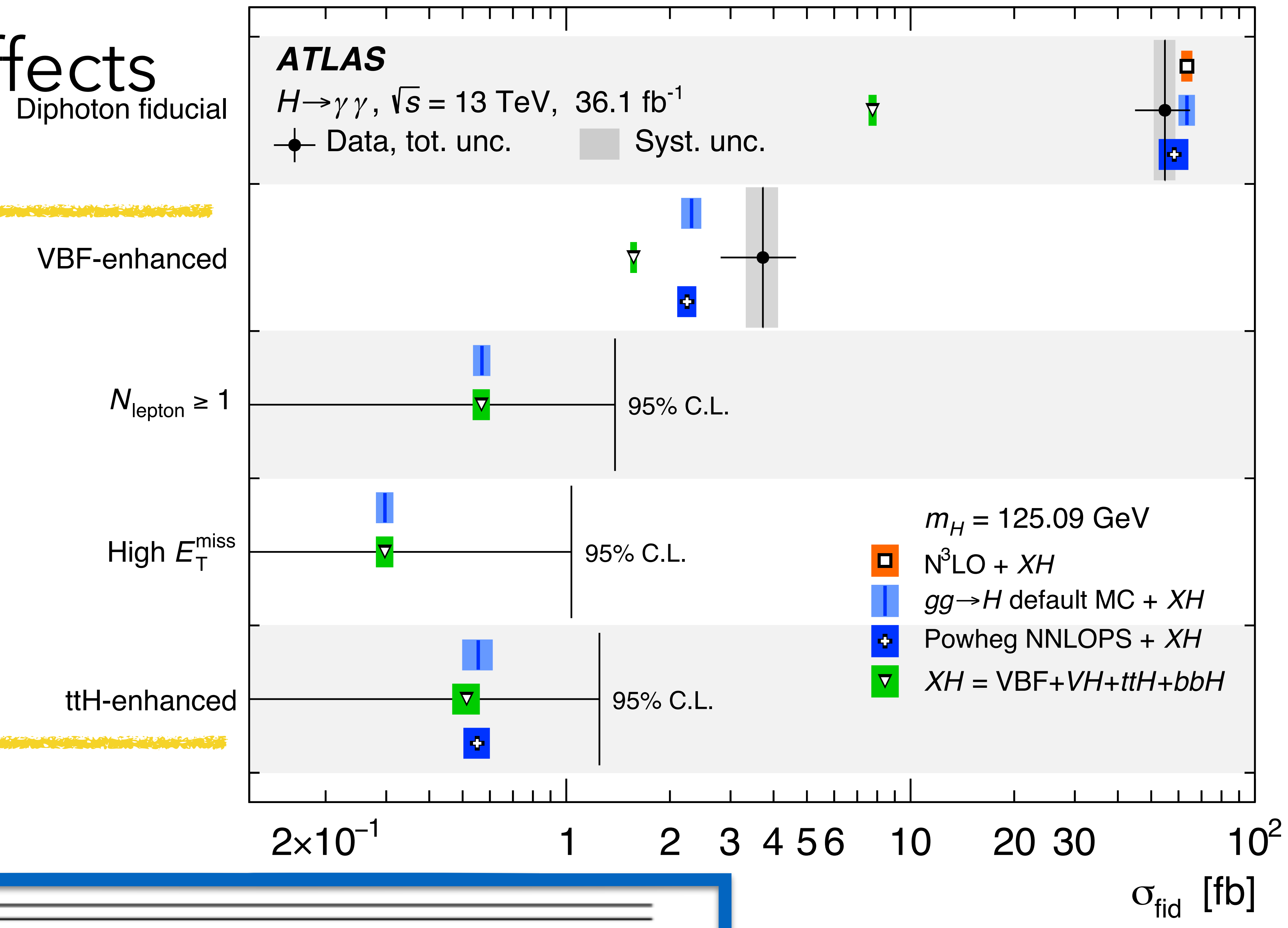

Fiducial region	Measured cross section	SM prediction	
Diphoton fiducial	55 ± 9 (stat.) ± 4 (exp.) ± 0.1 (theo.) fb	64 ± 2 fb	[N^{3}LO + XH]
VBF-enhanced	3.7 ± 0.8 (stat.) ± 0.5 (exp.) ± 0.2 (theo.) fb	2.3 ± 0.1 fb	[default MC + XH]
$N_{lepton} \geq 1$	≤ 1.39 fb 95% CL	0.57 ± 0.03 fb	[default MC + XH]
High E_T^{miss}	≤ 1.00 fb 95% CL	0.30 ± 0.02 fb	[default MC + XH]
$t\bar{t}H$-enhanced	≤ 1.27 fb 95% CL	0.55 ± 0.06 fb	[default MC + XH]

Compatible with SM predictions

JHEP 03 (2018) 095

H→ZZ*→4ℓ Production cross-section

- High resolution on Higgs mass, main background from non-resonant ZZ production, while other bkg. (Z + jets, top) strongly suppressed by selection
- Reconstructed events are classified into several exclusive **categories** based on the presence of jets and additional leptons in the final state
- **BDT discriminants** are introduced to increase the sensitivity of the cross-section measurements in the production bins

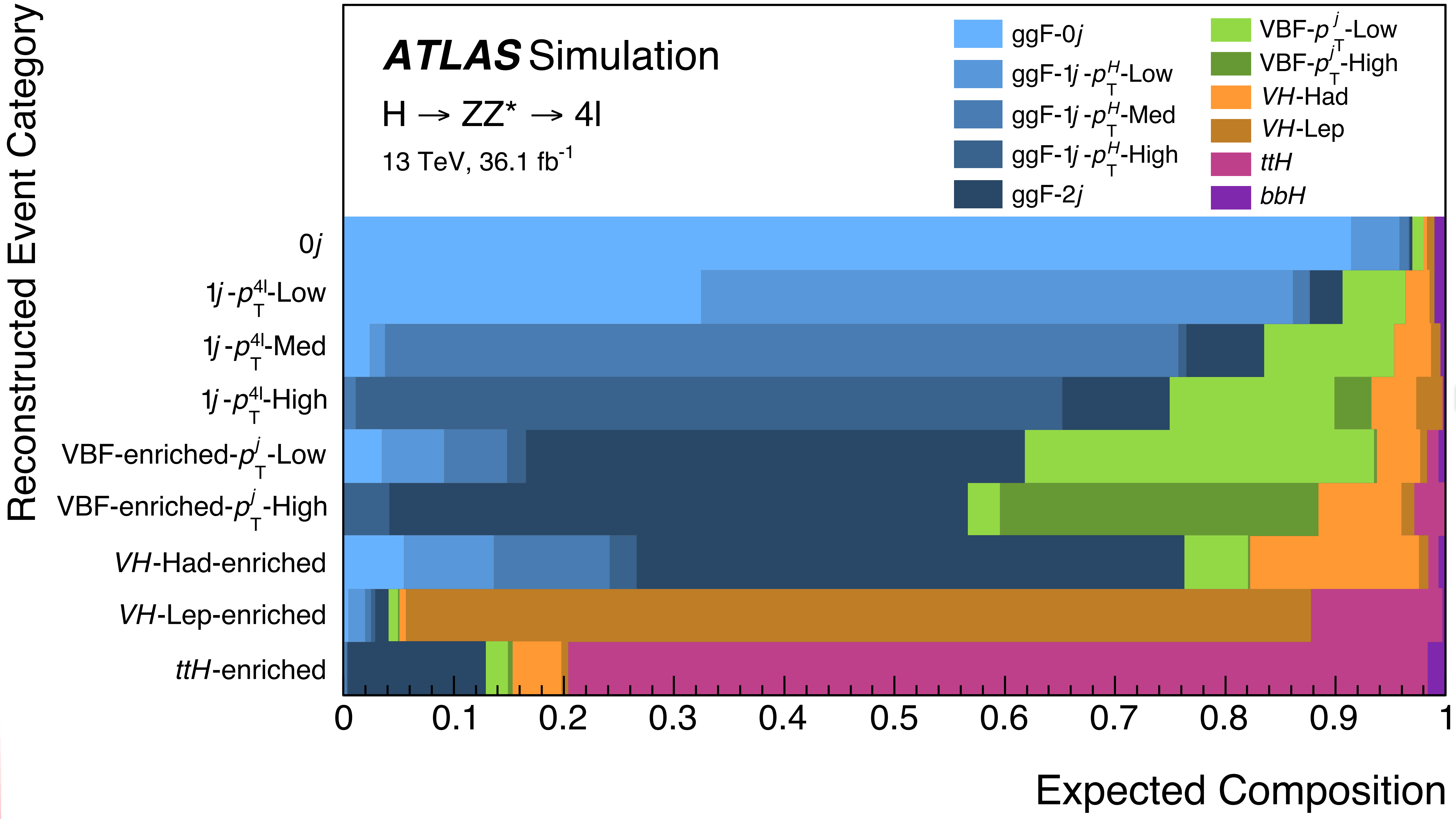

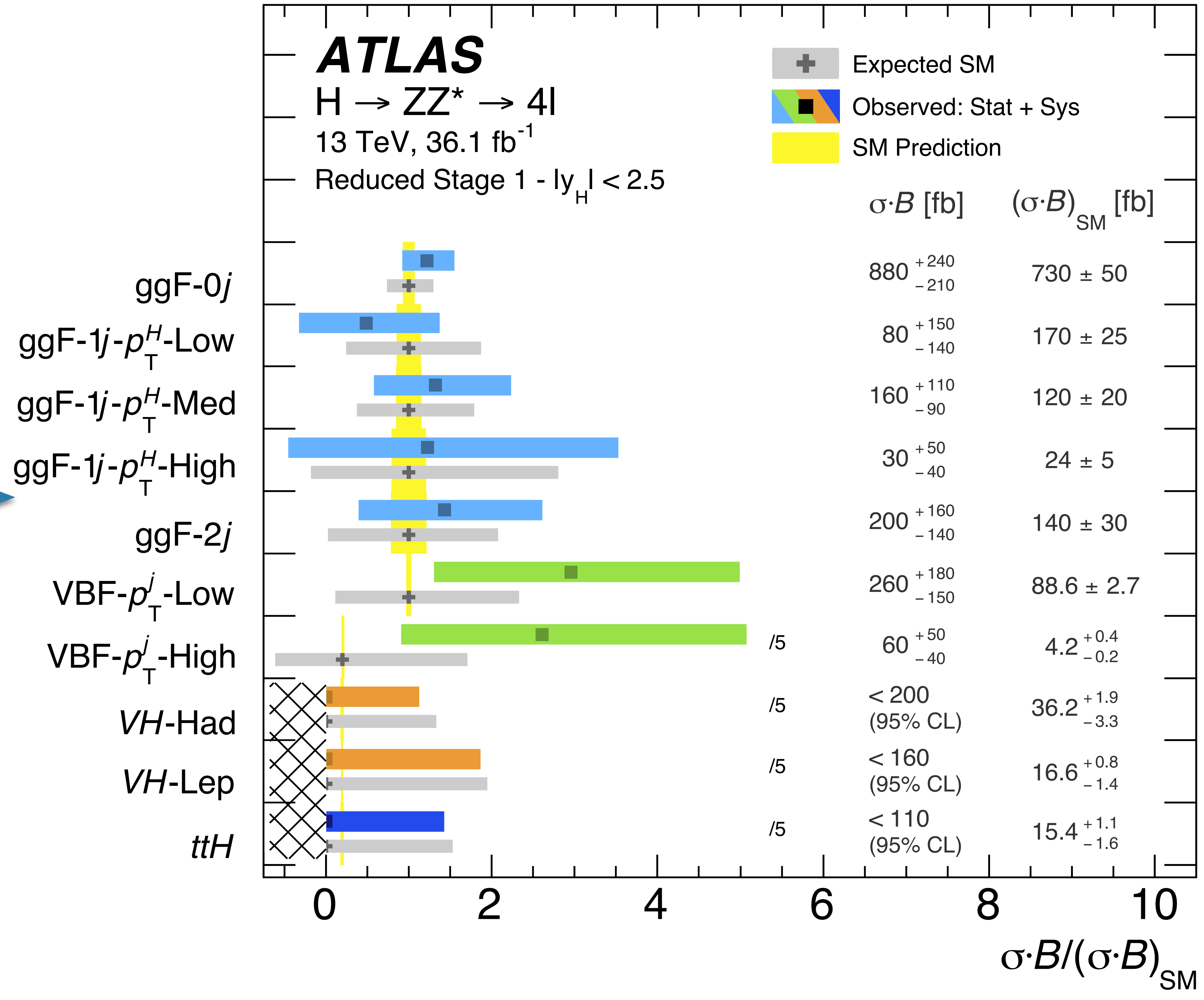

JHEP 10 (2017) 132

H→ZZ*→4ℓ Fiducial and differential cross-section

Invariant mass templates for the signal and the bkg processes are fit to the $m_{4\ell}$ distribution in data to extract N_{sig} in each bin of a differential distribution or for each decay channel

Measured inclusive fiducial cross-section in good agreement with SM prediction

$$\sigma_{fid,comb} = 3.62 \pm 0.50\ (\text{stat})\ {}^{+0.25}_{-0.20}\ (\text{sys})\ \text{fb}$$

$$\sigma_{fid,SM} = 2.91 \pm 0.13\ \text{fb}$$

(1.3σ difference in mixed channels)

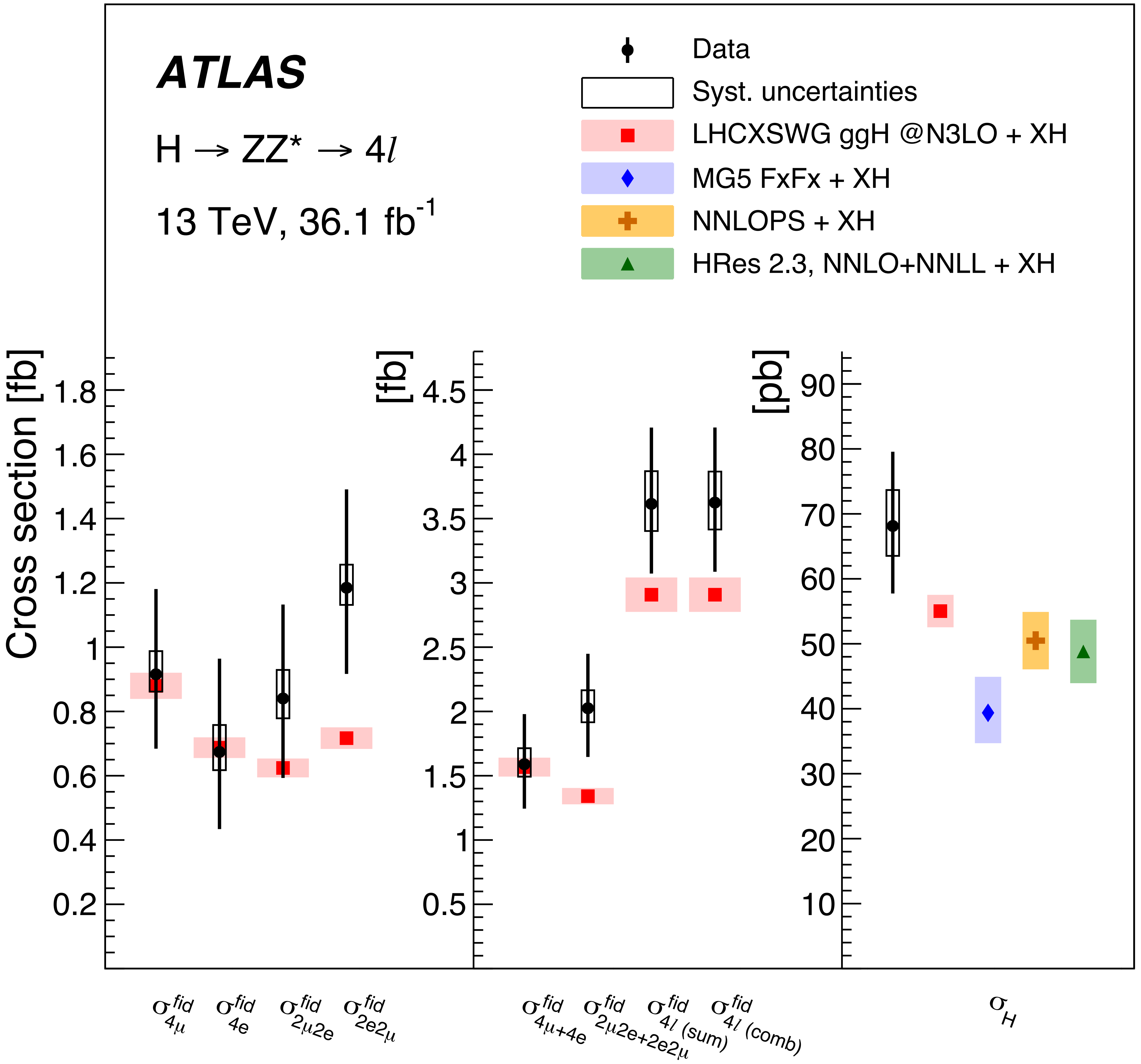

Differential distributions are sensitive to perturbative QCD calculations and presence of new particles in loops

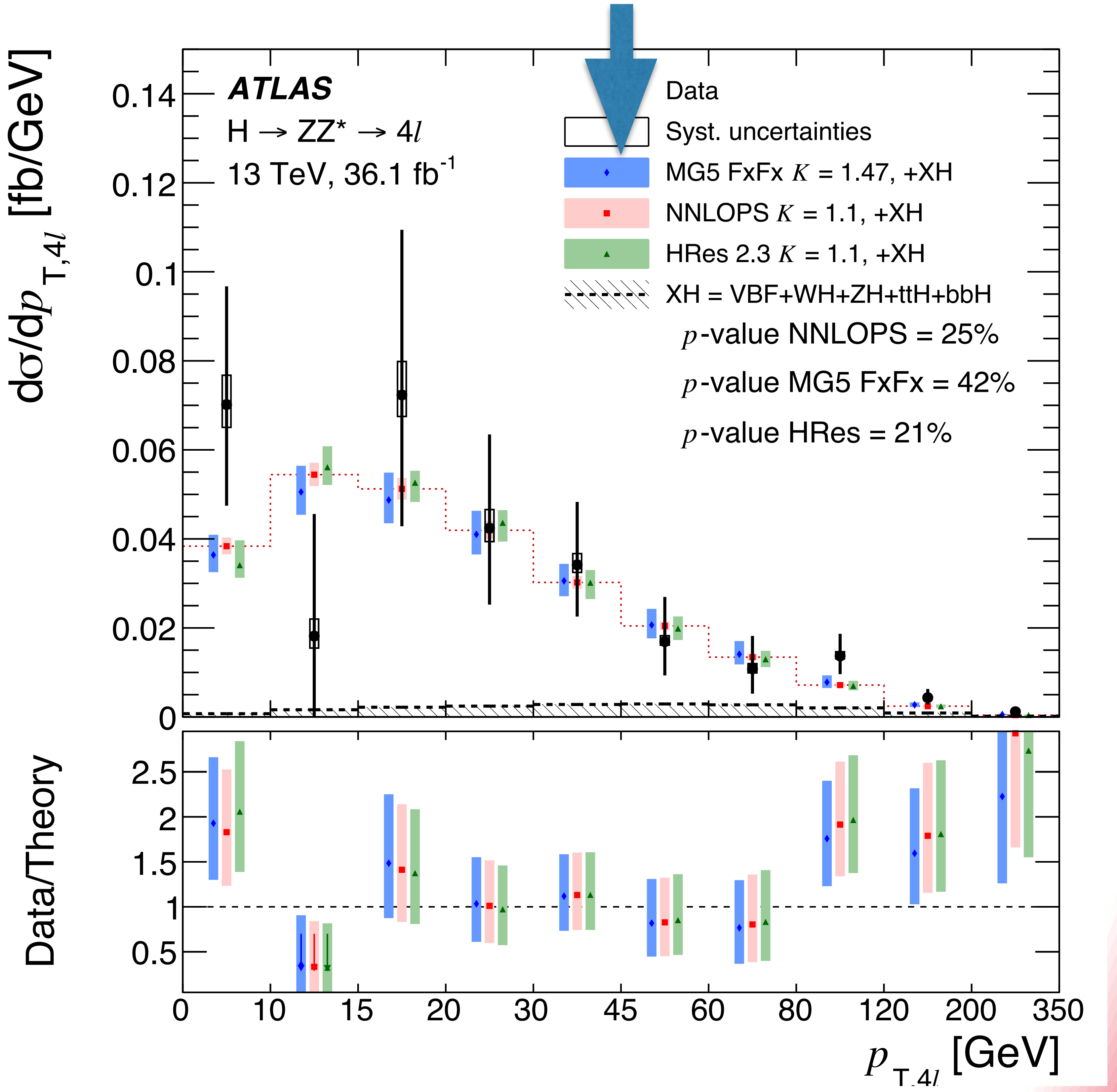

Total Higgs boson cross-section: H4ℓ, Hγγ combination

Combining H→4ℓ and H→γγ measurements to improve precision on Higgs boson cross-section

Combination is done in **total phase space** (more model-dependent)

Total cross section in good agreement with the SM predictions

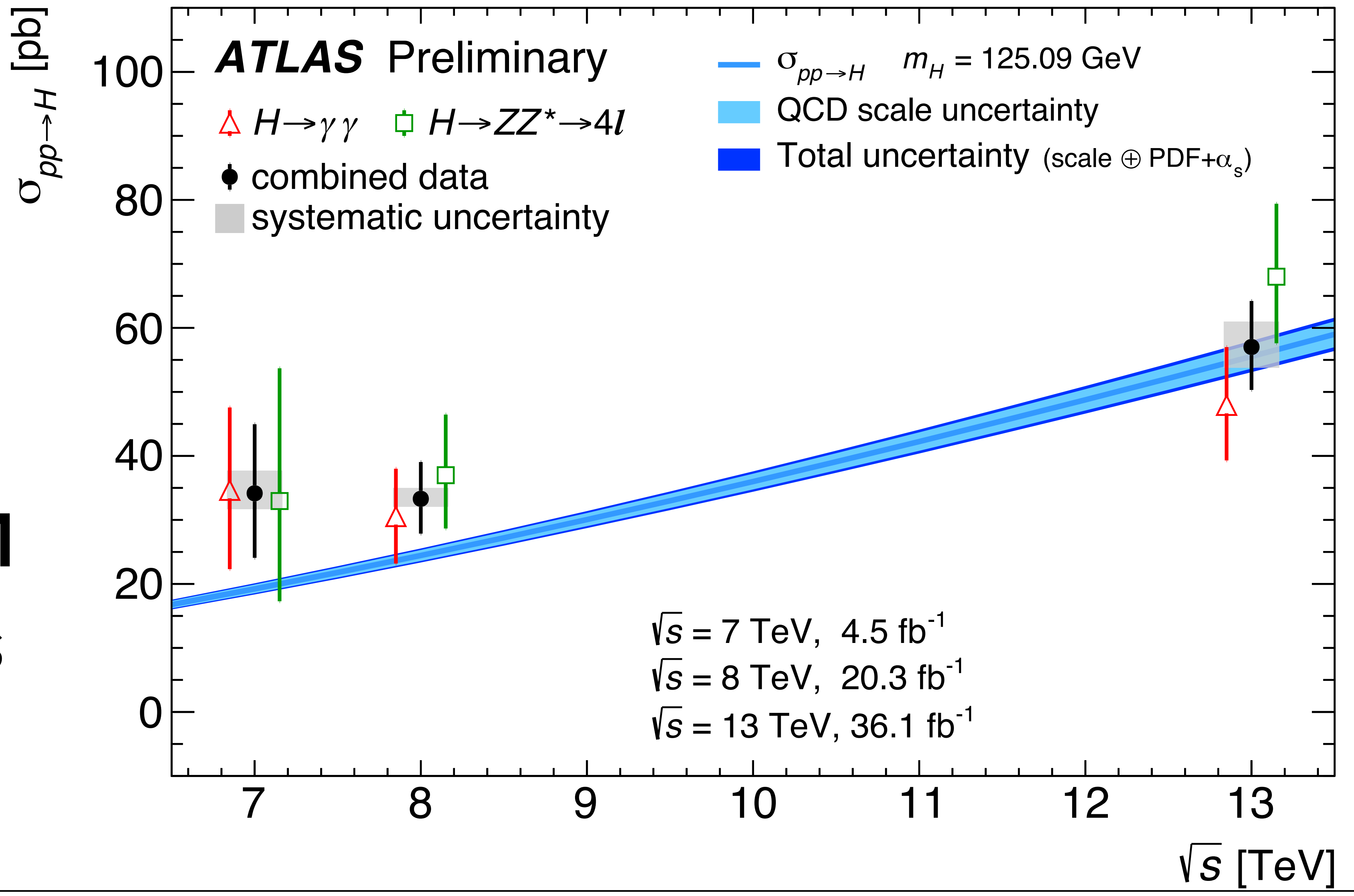

Decay channel	Total cross section ($pp \to H + X$)		
	$\sqrt{s}$ =7 TeV	$\sqrt{s}$ =8 TeV	$\sqrt{s}$ =13 TeV
$H \to \gamma\gamma$	35^{+13}_{-12} pb	$30.5^{+7.5}_{-7.4}$ pb	$47.9^{+9.1}_{-8.6}$ pb
$H \to ZZ^* \to 4\ell$	33^{+21}_{-16} pb	37^{+9}_{-8} pb	$68.0^{+11.4}_{-10.4}$ pb
Combination	34 ± 10 (stat.) $^{+4}_{-2}$ (syst.) pb	$33.3^{+5.5}_{-5.3}$ (stat.) $^{+1.7}_{-1.3}$ (syst.) pb	$57.0^{+6.0}_{-5.9}$ (stat.) $^{+4.0}_{-3.3}$ (syst.) pb
SM prediction [8]	19.2 ± 0.9 pb	24.5 ± 1.1 pb	$55.6^{+2.4}_{-3.4}$ pb

Single signal strength fit for all the production and decay modes

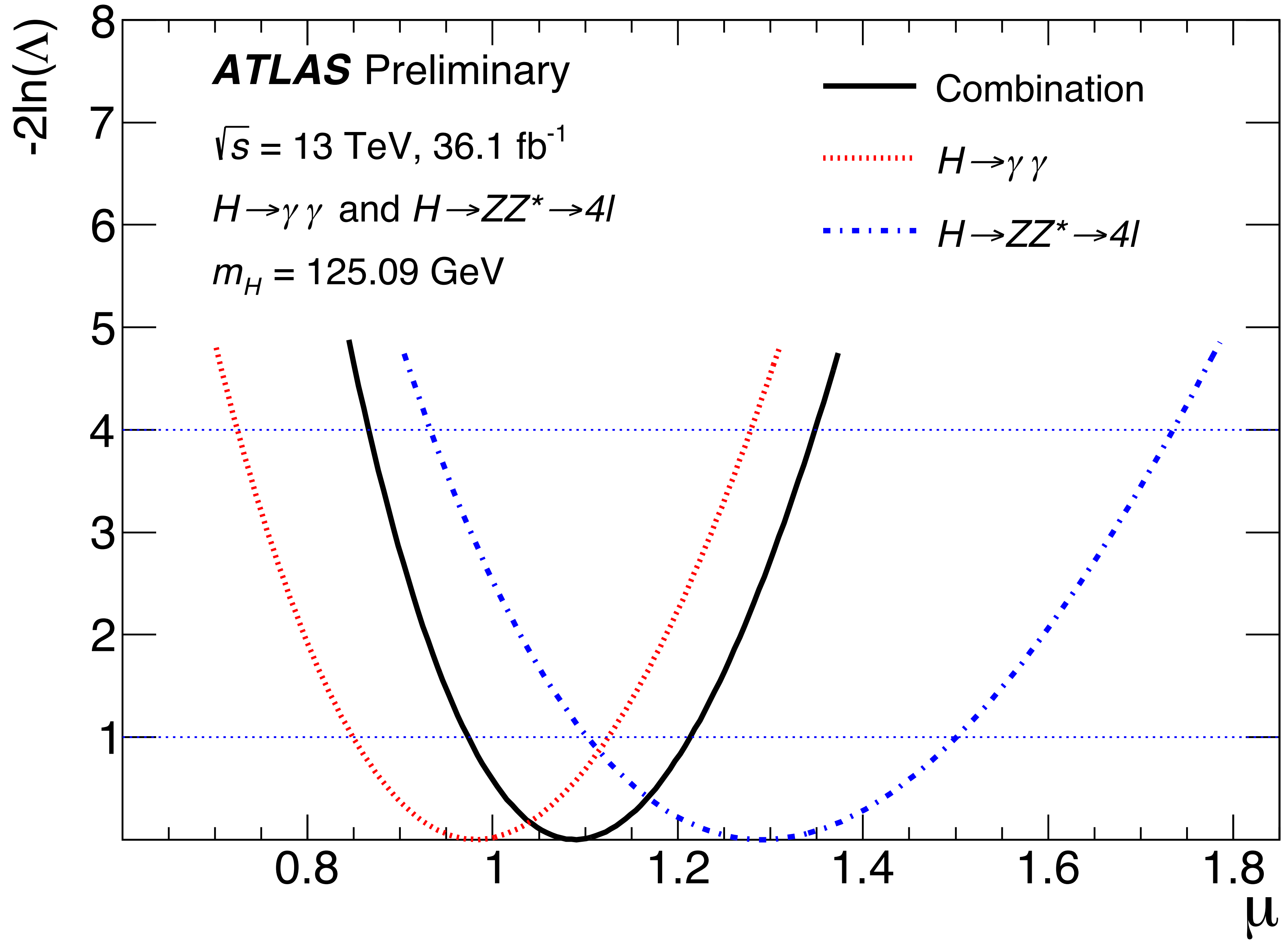

$$\mu = 1.09 \pm 0.12 = 1.09 \pm 0.09\,(\text{stat.})\,^{+0.06}_{-0.05}\,(\text{exp.})\,^{+0.06}_{-0.05}\,(\text{th.}).$$

Consistent with the SM prediction (p-value 47%)

ATLAS-CONF-2017-047

H4ℓ, Hγγ combined production mode cross-section

Combined H→4ℓ and H→γγ for |y(H)| < 2.5 in Higgs boson production categories: ggF, VBF, VH and ttH

Cross-sections and branching fractions expressed as ratios to cancel contributions from common systematic uncertainties

Quantity		Result	Uncertainty: Total	Stat.	Exp.	Th.	SM prediction
$\sigma_{\text{ggF}}\cdot \text{B}_{4\ell}$	[fb]	6.6	$^{+1.2}_{-1.0}$	$^{+1.1}_{-1.0}$	±0.4	±0.2	$5.6^{+0.3}_{-0.4}$
$\text{B}_{\gamma\gamma}/\text{B}_{4\ell}$		12.5	$^{+2.8}_{-2.3}$	$^{+2.6}_{-2.2}$	$^{+0.9}_{-0.7}$	±0.2	18.1 ± 0.2
$\sigma_{\text{VBF}}/\sigma_{\text{ggF}}$	$[10^{-2}]$	21.5	$^{+8.5}_{-6.3}$	$^{+7.3}_{-5.6}$	$^{+2.8}_{-1.7}$	$^{+3.6}_{-2.2}$	$7.9^{+0.4}_{-0.6}$
$\sigma_{VH}/\sigma_{\text{ggF}}$	$[10^{-2}]$	0.2	$^{+4.5}_{-3.4}$	$^{+4.2}_{-3.2}$	$^{+1.2}_{-0.9}$	$^{+0.9}_{-0.4}$	$4.5^{+0.2}_{-0.3}$
$\sigma_{t\bar{t}H}/\sigma_{\text{ggF}}$	$[10^{-2}]$	0.7	$^{+1.0}_{-0.9}$	$^{+1.0}_{-0.9}$	$^{+0.2}_{-0.1}$	±0.1	1.3 ± 0.1

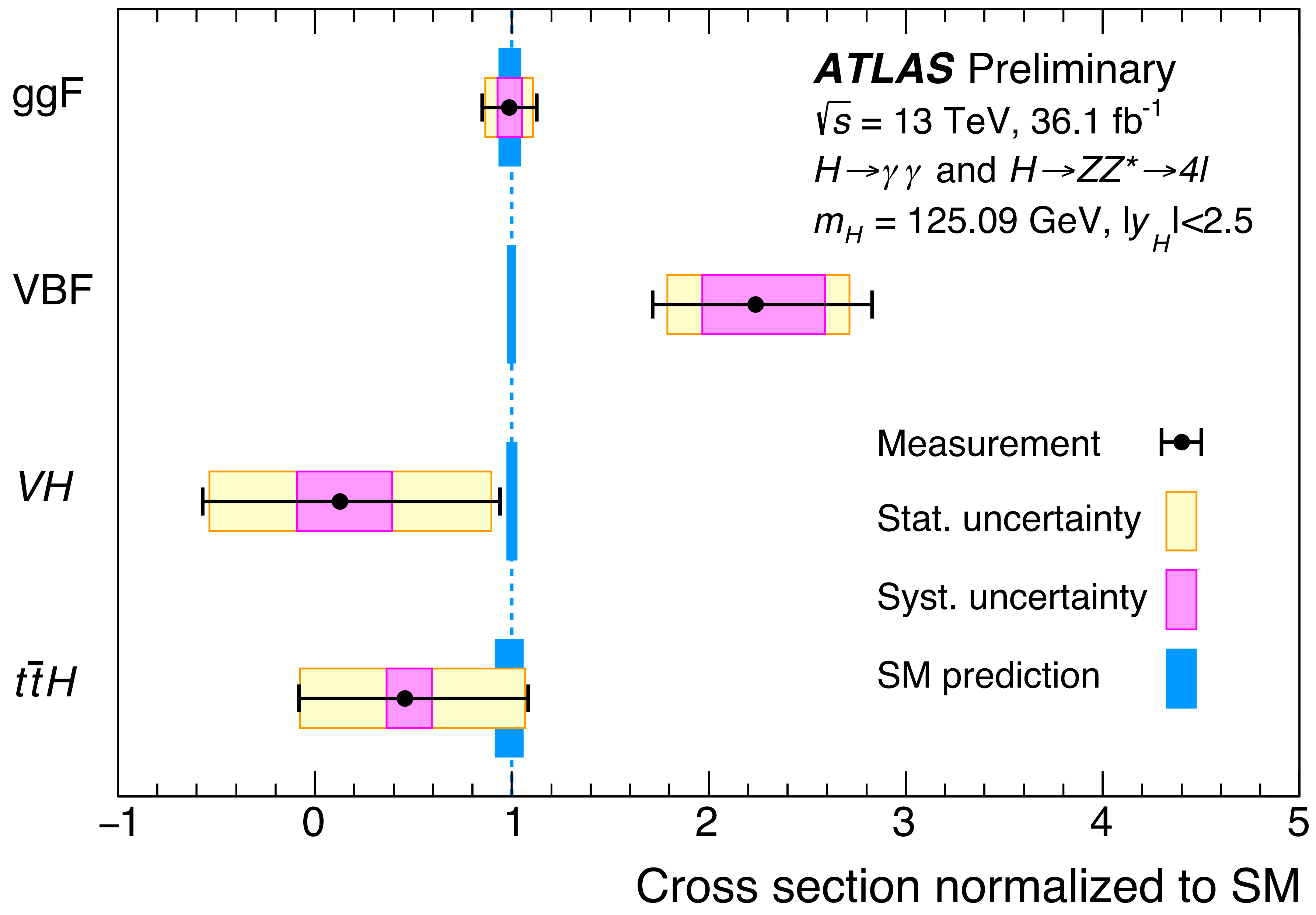

Simplified template cross sections:

Exclusive kinematic regions targeting specific production modes are defined to reduce model dependance

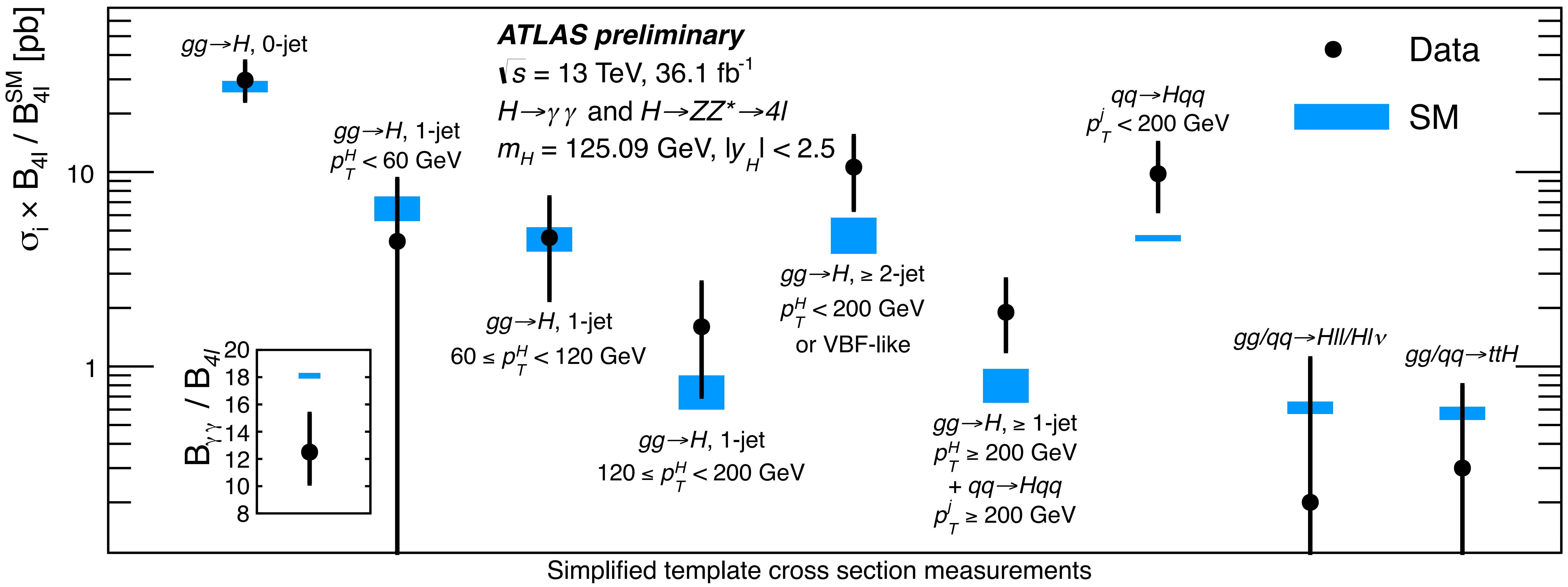

L. S. Bruni

H4ℓ, Hγγ combination - couplings

Cross section results by production mode of the H→ZZ*→4l and H→γγ combination can be interpreted within the **κ framework**

$$\sigma(i \to H \to f) = \kappa_i^2 \sigma_i^{\mathrm{SM}} \frac{\kappa_f^2 \Gamma_f^{\mathrm{SM}}}{\kappa_H^2 \Gamma_H^{\mathrm{SM}}}$$

➡Coupling modifiers κ_V and κ_F, to probe the Higgs couplings with the SM bosons and fermions

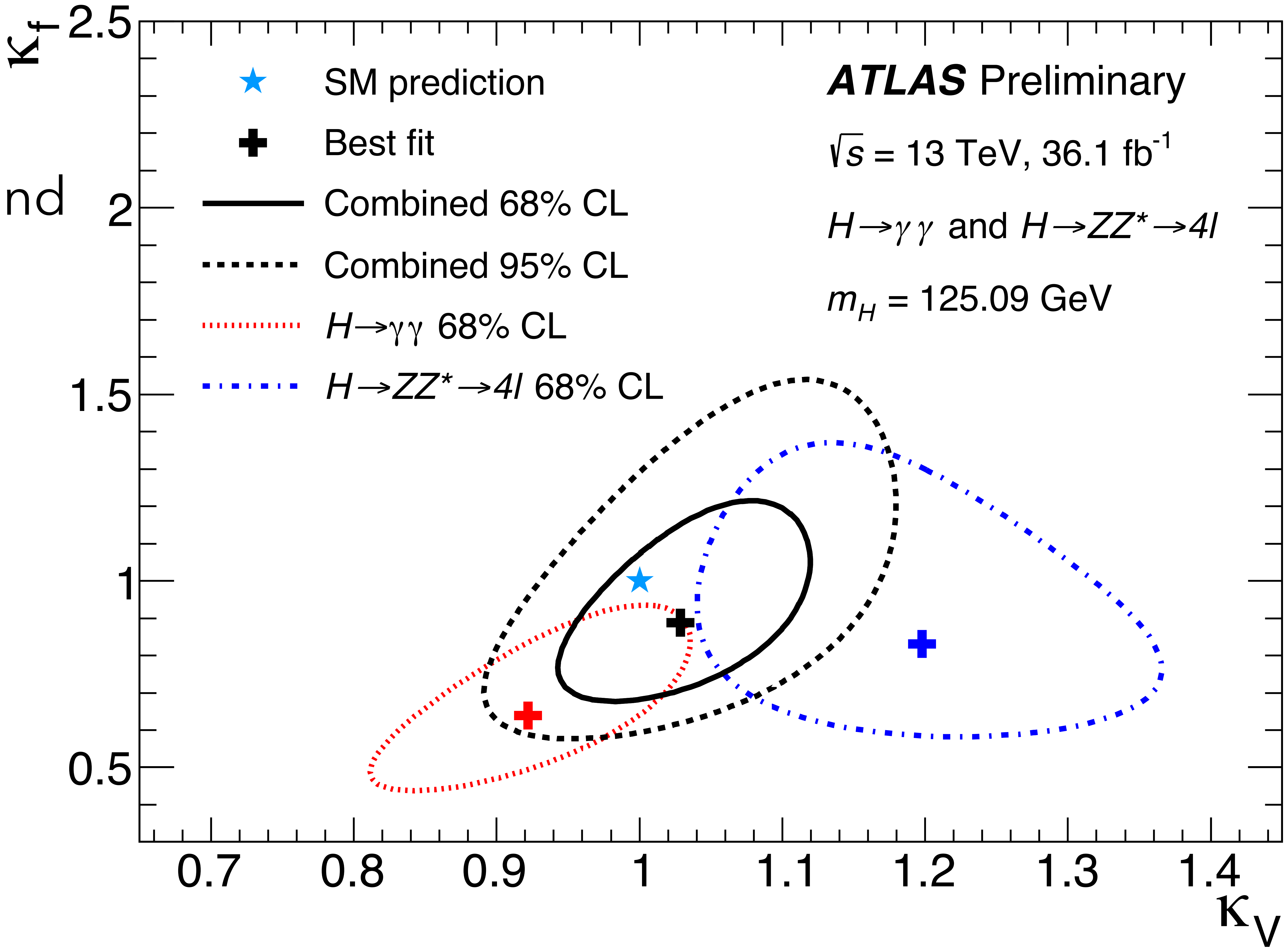

Measurements consistent with the SM predictions within the experimental uncertainties

Probing spin and CP

arXiv:1802.04146v1
ATLAS-CONF-2018-002

Higgs spin/CP properties probed in both $H\to\gamma\gamma$ and $H\to ZZ*\to 4\ell$ channels with differential distributions

$\Delta\phi_{jj}$

azimuthal angle between the two leading jets

Sensitive to CP

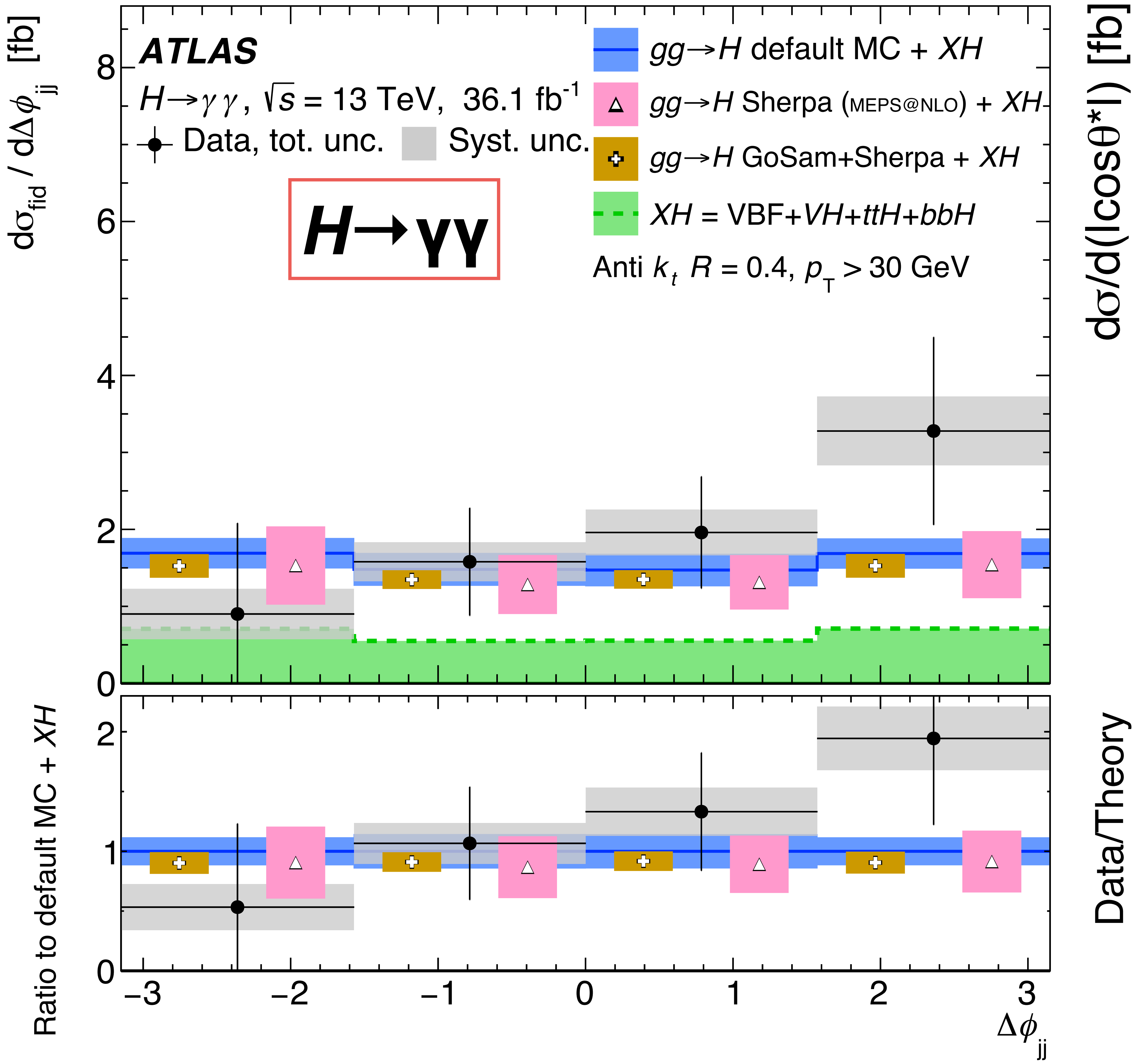

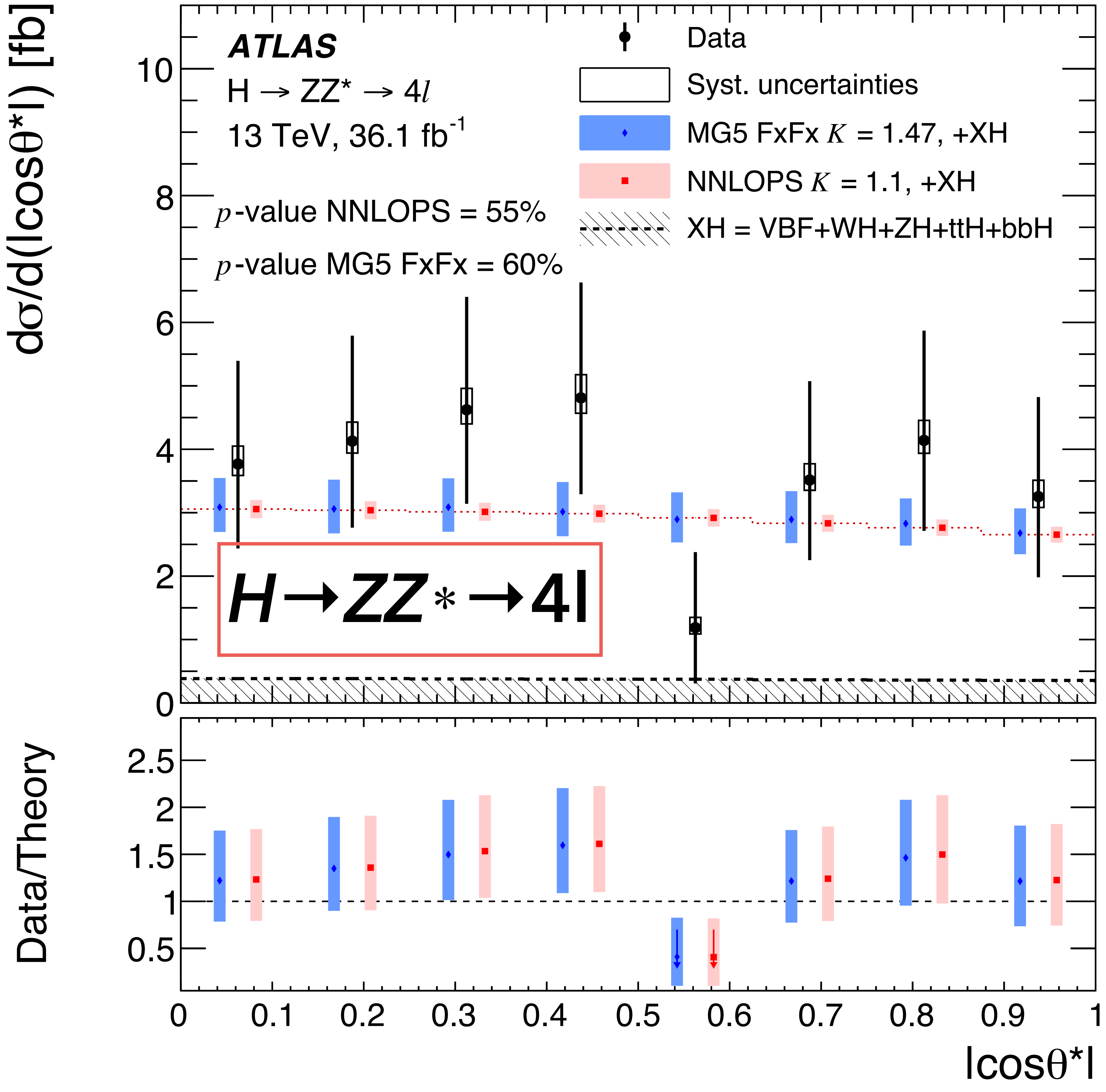

$|\cos\theta^*|$

absolute value of the cosine of the angle between the beam axis and the two Z in the Higgs rest frame

Sensitive to spin

Consistent with SM predictions for a CP-even scalar particle.

Conclusions

- Overview of the ATLAS latest results with Higgs boson decaying into vectors bosons using 36.1 fb^{-1} of Run 2 data
- Precision era for Higgs boson measurements has started
- Results shown in terms of (fiducial) integrated and differential cross-sections, couplings and Higgs boson properties (mass, spin-parity)
- The new results obtained in Run 2 measurements are consistent with the SM predictions
- Some results are still limited by statistics, but more data is to be analysed!
- Looking forward to Run 2 full dataset:
  - ➡New ~45 fb^{-1} recorded during 2017 data-taking still to be analysed
  - ➡More data expected at the end of Run 2!

Back-up

Higgs production modes

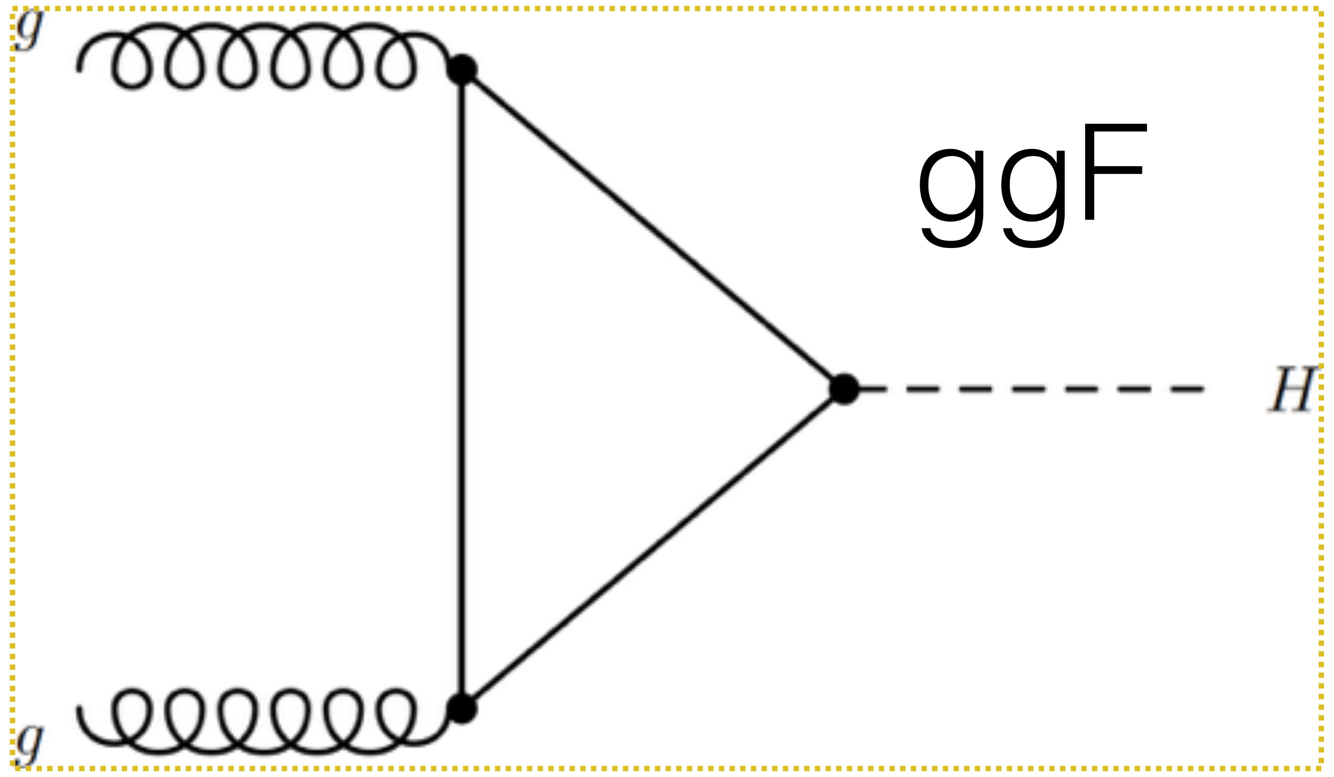

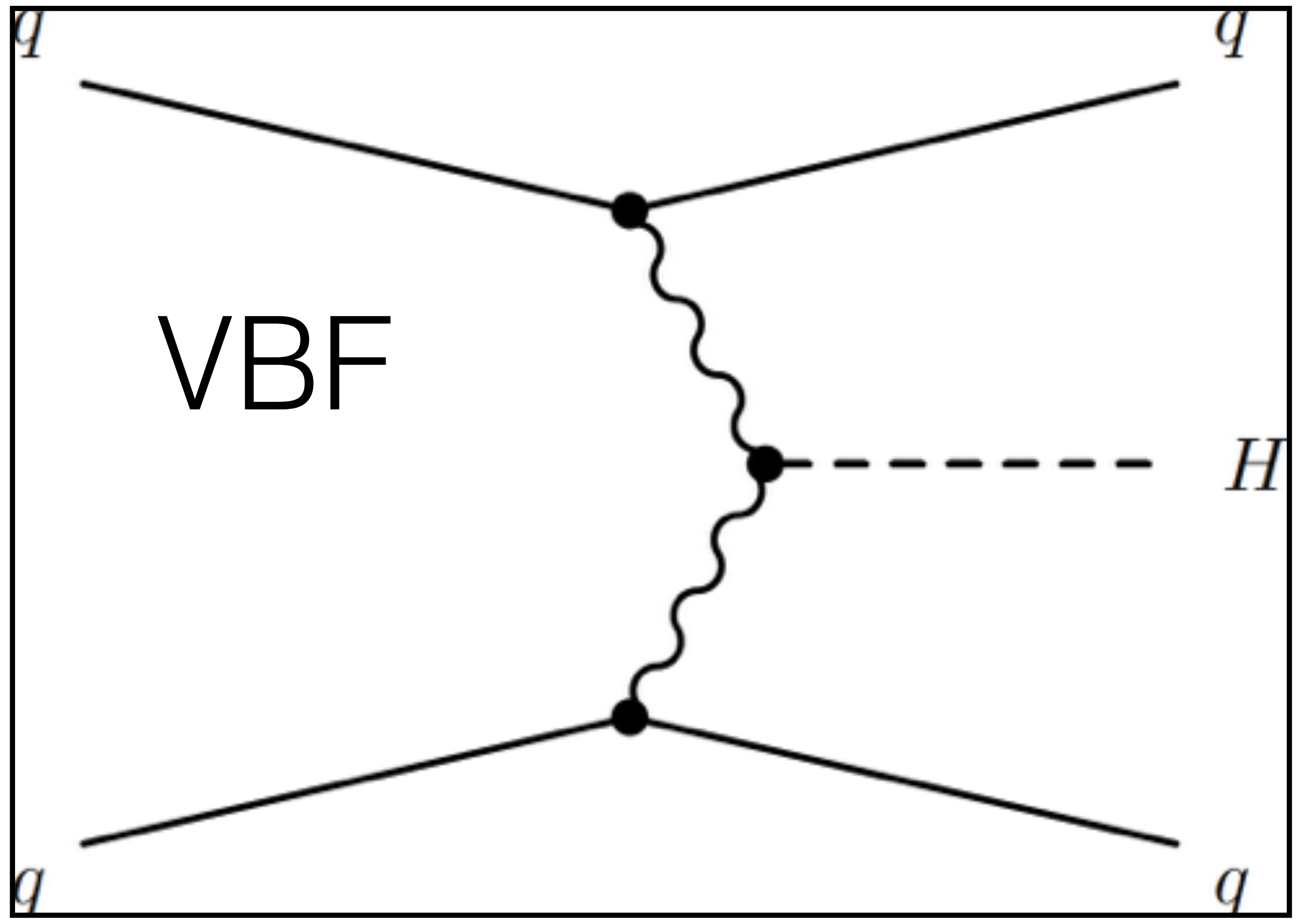

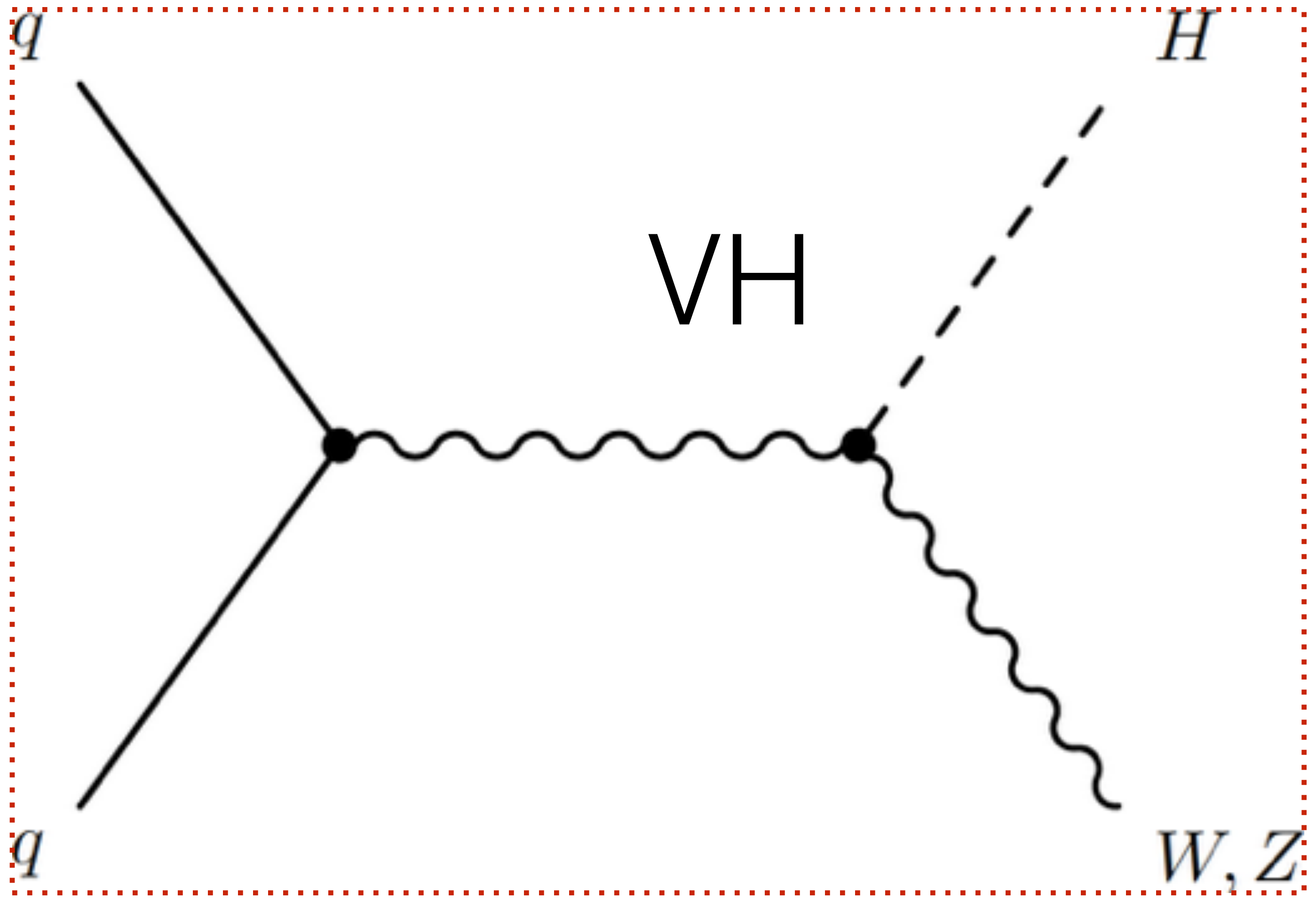

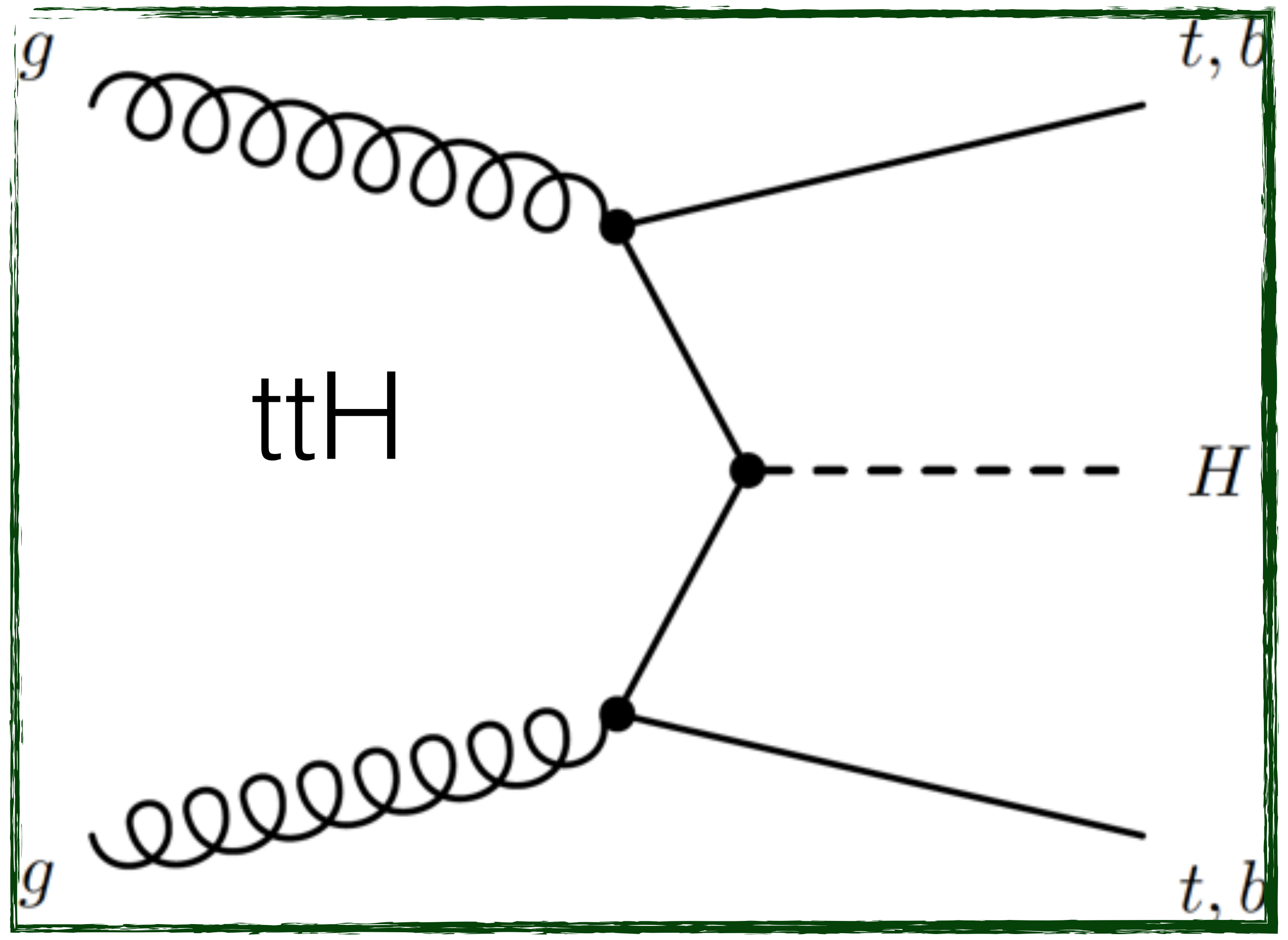

H→WW*→eνμν analysis

SR selection

<table>
<tr><th>Category</th><th>$N_{\text{jet}} = 0$</th><th>$N_{\text{jet}} = 1$</th><th>$N_{\text{jet}} \geq 2$, VBF</th></tr>
<tr><td>Preselection</td><td colspan="3">Two isolated, different-flavour, leptons ($\ell = e, \mu$) with opposite charge
$p_{\mathrm{T}}^{\text{lead}} > 22$ GeV , $p_{\mathrm{T}}^{\text{sublead}} > 15$ GeV
$m_{\ell\ell} > 10$ GeV</td></tr>
<tr><td></td><td colspan="2">$E_{\mathrm{T}}^{\text{miss, track}} > 20$ GeV</td><td></td></tr>
<tr><td rowspan="3">Background rejection</td><td colspan="3">$N_{b\text{-jet},(p_{\mathrm{T}}>20\text{ GeV})} = 0$</td></tr>
<tr><td>$\Delta\phi(\ell\ell, E_{\mathrm{T}}^{\text{miss}}) > \pi/2$
$p_{\mathrm{T}}^{\ell\ell} > 30$ GeV</td><td>$\max\left(m_{\mathrm{T}}^{\ell}\right) > 50$ GeV</td><td></td></tr>
<tr><td></td><td colspan="2">$m_{\tau\tau} < m_Z - 25$ GeV</td></tr>
<tr><td>$H \to WW^* \to e\nu\mu\nu$ topology</td><td colspan="2">$m_{\ell\ell} < 55$ GeV
$\Delta\phi_{\ell\ell} < 1.8$</td><td>Central Jet Veto
Outside Lepton Veto</td></tr>
<tr><td>Discriminant Variable
BDT input variables</td><td colspan="2">m_{T}</td><td>BDT
$m_{jj}, \Delta y_{jj}, m_{\ell\ell}, \Delta\phi_{\ell\ell}, m_{\mathrm{T}}, \sum C_{\ell}, \sum_{\ell,j} m_{\ell j}, p_{\mathrm{T}}^{\text{tot}}$</td></tr>
</table>

CR selection

<table>
<tr><th>CR</th><th>$N_{\text{jet}} = 0$</th><th>$N_{\text{jet}} = 1$</th><th>$N_{\text{jet}} \geq 2$, VBF</th></tr>
<tr><td rowspan="3">WW</td><td>$55 < m_{\ell\ell} < 110$ GeV
$\Delta\phi_{\ell\ell} < 2.6$</td><td>$m_{\ell\ell} > 80$ GeV
$|m_{\tau\tau} - m_Z| > 25$ GeV</td><td rowspan="3"></td></tr>
<tr><td colspan="2">b-jet veto</td></tr>
<tr><td></td><td>$m_{\mathrm{T}}^{\ell} > 50$ GeV</td></tr>
<tr><td rowspan="2">Top-quark</td><td rowspan="2">$N_{b\text{-jet},(20\text{ GeV}<p_{\mathrm{T}}<30\text{ GeV})} > 0$
$\Delta\phi(\ell\ell, E_{\mathrm{T}}^{\text{miss}}) > \pi/2$
$p_{\mathrm{T}}^{\ell\ell} > 30$ GeV
$\Delta\phi_{\ell\ell} < 2.8$</td><td>$N_{b\text{-jet},(p_{\mathrm{T}}>30\text{ GeV})} = 1$
$N_{b\text{-jet},(20\text{ GeV}<p_{\mathrm{T}}<30\text{ GeV})} = 0$
$\max\left(m_{\mathrm{T}}^{\ell}\right) > 50$ GeV</td><td>$N_{b\text{-jet},(p_{\mathrm{T}}>20\text{ GeV})} = 1$
Central Jet Veto</td></tr>
<tr><td colspan="2">$m_{\tau\tau} < m_Z - 25$ GeV
Outside Lepton Veto</td></tr>
<tr><td rowspan="3">$Z \to \tau\tau$</td><td colspan="2">no $E_{\mathrm{T}}^{\text{miss, track}}$ requirement
$m_{\ell\ell} < 80$ GeV</td><td>Outside Lepton Veto
Central Jet Veto</td></tr>
<tr><td>$\Delta\phi_{\ell\ell} > 2.8$</td><td colspan="2">$m_{\tau\tau} > m_Z - 25$ GeV</td></tr>
<tr><td></td><td colspan="2">$N_{b\text{-jet},(p_{\mathrm{T}}>20\text{ GeV})} = 0$</td></tr>
</table>

H→WW*→eνμν analysis

Source	$\frac{\Delta\sigma_{\mathrm{ggF}}}{\sigma_{\mathrm{ggF}}}$ [%]	$\frac{\Delta\sigma_{\mathrm{VBF}}}{\sigma_{\mathrm{VBF}}}$ [%]
Data statistics	±8	±46
CR statistics	±8	±9
MC statistics	±5	±23
Theoretical uncertainties	±8	±21
ggF signal	±5	±15
VBF signal	<1	±15
WW	±5	±12
Top-quark	±4	±4
Experimental uncertainties	±9	±8
b-tagging	±5	±6
Pile-up	±5	±2
Jet	±3	±4
Electron	±3	<1
Misidentified leptons	±5	±9
Luminosity	±2	±3
TOTAL	±17	±59

Process	$N_{\mathrm{jet}} = 0$ SR	$N_{\mathrm{jet}} = 1$ SR	$N_{\mathrm{jet}} \geq 2$ VBF SR
ggF	680 ± 110	303 ± 52	37 ± 13
VBF	6.8 ± 0.8	30.0 ± 1.9	30 ± 16
WW	2960 ± 670	1020 ± 390	386 ± 59
VV	323 ± 34	204 ± 30	71 ± 14
$t\bar{t}/Wt$	580 ± 128	1400 ± 180	1234 ± 89
Mis-Id	471 ± 80	246 ± 50	109 ± 38
Z/γ^*	27 ± 10	76 ± 22	298 ± 42
Total	5062 ± 67	3290 ± 51	2138 ± 47
Observed	5089	3264	2164

arXiv:1802.04146v1

H→γγ - Couplings

Table 7: Expected and observed significances of the VBF, VH and top quark associated production mode signal strengths.

Measurement	Exp. Z_0	Obs. Z_0
μ_{VBF}	2.6 σ	4.9 σ
μ_{VH}	1.4 σ	0.8 σ
μ_{top}	1.8 σ	1.0 σ

Table 8: Observed and expected upper limits at 95% CL on the signal strengths μ_{VH} and μ_{top}. The median expected limits are given for either the case when the true value of the signal strength under study is the SM value ($\mu_i = 1$) or zero. The $\pm 1\ \sigma$ and $\pm 2\ \sigma$ intervals for the expected upper limit in the case $\mu_i = 0$ are also reported.

Measurement	Observed	Exp. Limit ($\mu_i = 1$)	Exp. Limit ($\mu_i = 0$)	$+2\sigma$	$+1\sigma$	-1σ	-2σ
μ_{VH}	2.3	2.5	1.5	3.1	2.2	1.1	0.8
μ_{top}	1.7	2.3	1.2	2.6	1.8	0.9	0.6

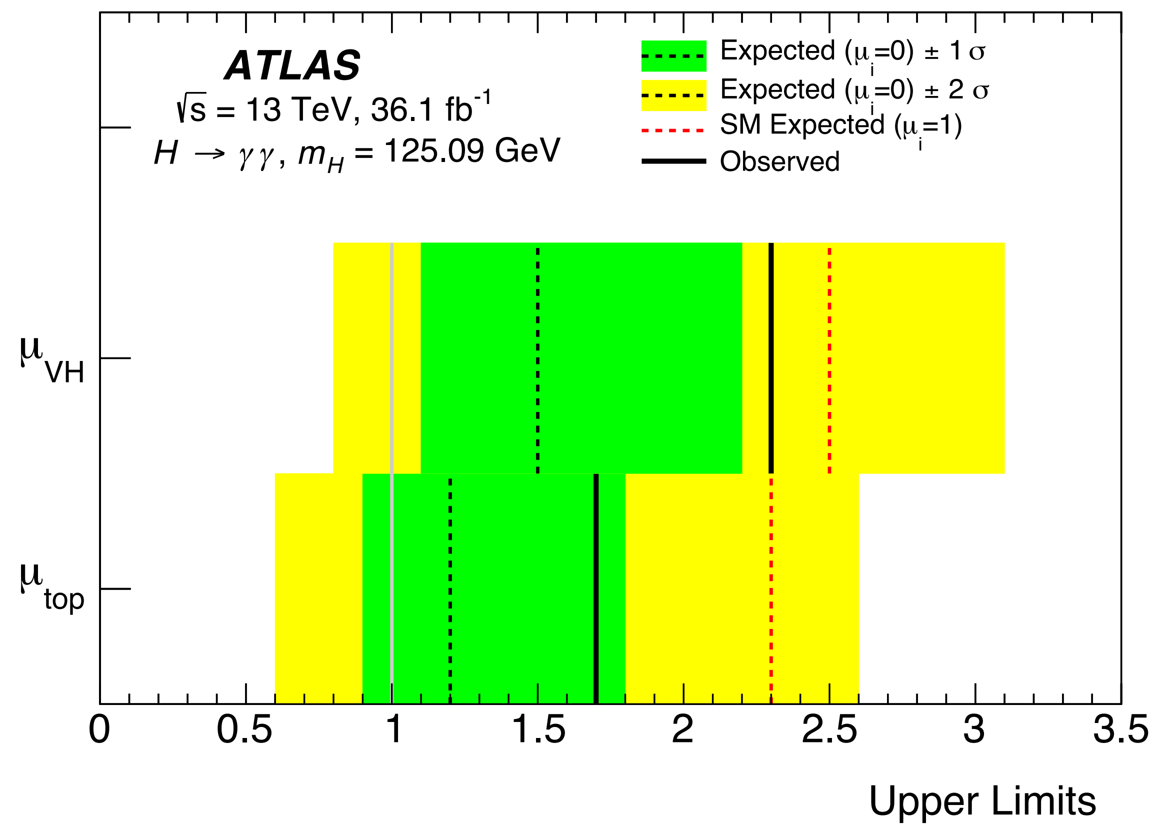

Uncertainty Group	$\sigma_{\mu}^{\mathrm{syst.}}$
Theory (QCD)	0.041
Theory ($B(H \to \gamma\gamma)$)	0.028
Theory (PDF+α_S)	0.021
Theory (UE/PS)	0.026
Luminosity	0.031
Experimental (yield)	0.017
Experimental (migrations)	0.015
Mass resolution	0.029
Mass scale	0.006
Background shape	0.027

arXiv:1802.04146v1

H→γγ - Simplified Template Cross Section

With current data no sensitivity to all the STXS stage-1 31 categories → fit in performed in10 phase space regions obtained from merging the initial 31

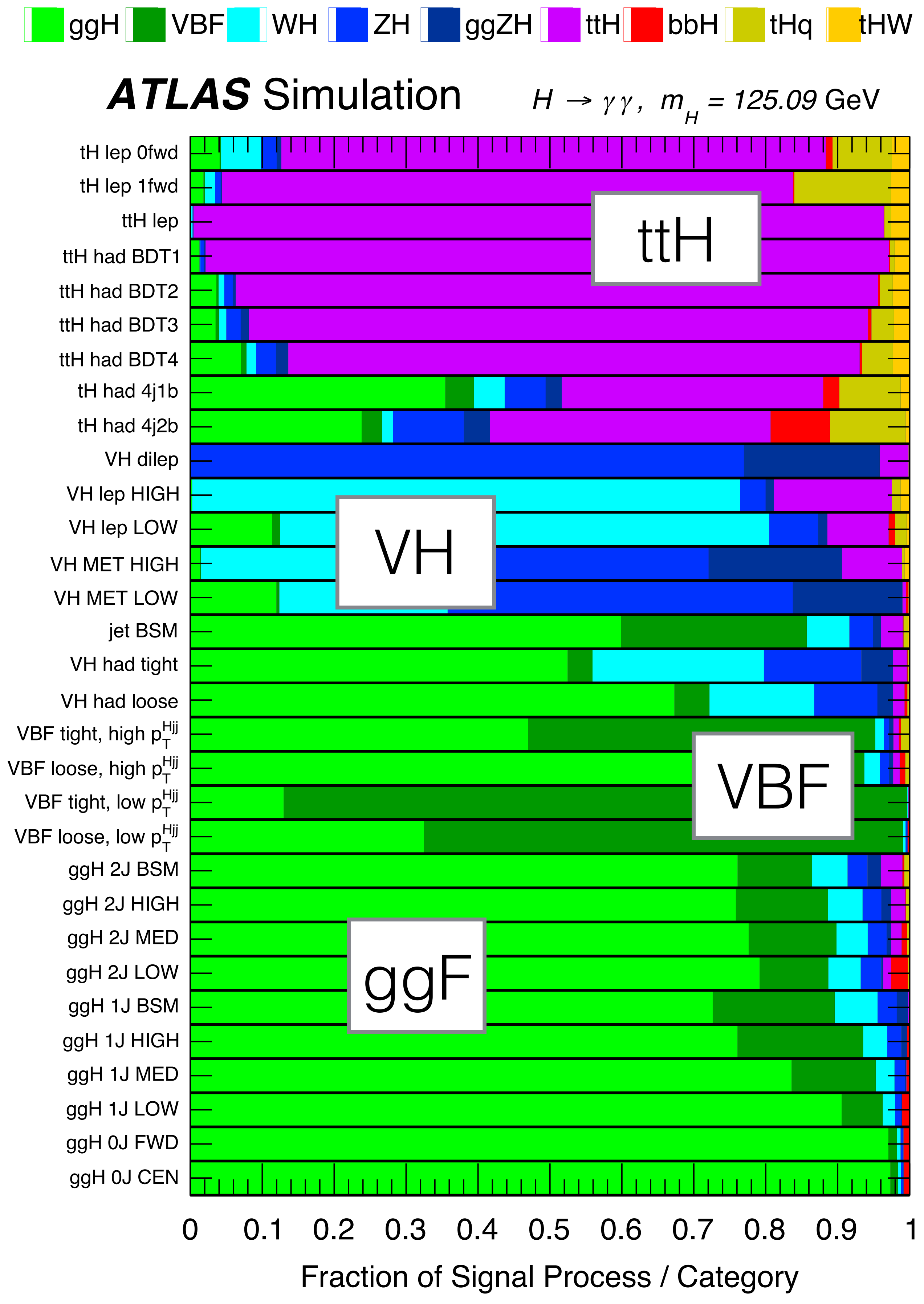

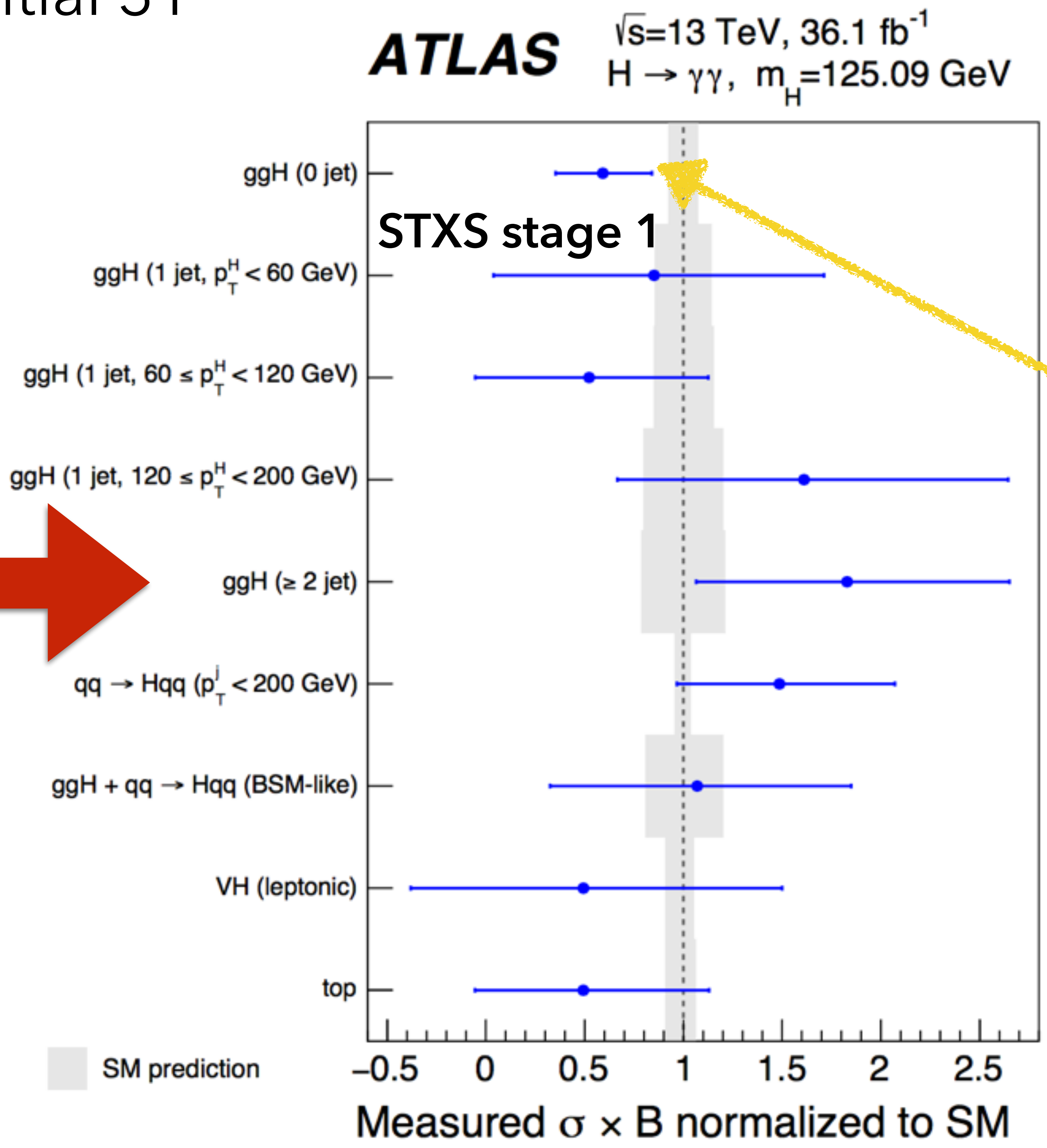

largest deviation (1.7 σ) from the SM in the ggH,0 jets bin

All observed cross sections are in agreement with the Standard Model values

H→γγ - MC

arXiv:1802.04146v1

Process	Generator	Showering	PDF set	σ [pb] $\sqrt{s}$ = 13 TeV	Order of calculation of σ
ggH	Powheg NNLOPS	Pythia8	PDF4LHC15	48.52	$\mathrm{N^3LO(QCD)+NLO(EW)}$
VBF	Powheg-Box	Pythia8	PDF4LHC15	3.78	NNLO(QCD)+NLO(EW)
WH	Powheg-Box	Pythia8	PDF4LHC15	1.37	NNLO(QCD)+NLO(EW)
$q\bar{q}' \to ZH$	Powheg-Box	Pythia8	PDF4LHC15	0.76	NNLO(QCD)+NLO(EW)
$gg \to ZH$	Powheg-Box	Pythia8	PDF4LHC15	0.12	NLO+NLL(QCD)
$t\bar{t}H$	MG5_aMC@NLO	Pythia8	NNPDF3.0	0.51	NLO(QCD)+NLO(EW)
$b\bar{b}H$	MG5_aMC@NLO	Pythia8	CT10	0.49	5FS(NNLO)+4FS(NLO)
t-channel tH	MG5_aMC@NLO	Pythia8	CT10	0.07	4FS(LO)
W-associated tH	MG5_aMC@NLO	Herwig++	CT10	0.02	5FS(NLO)
$\gamma\gamma$	Sherpa	Sherpa	CT10		
$V\gamma\gamma$	Sherpa	Sherpa	CT10		

The gluon–gluon fusion part of the SM prediction is constructed from the NNLOPS prediction for ggf normalized with the $\mathrm{N^3LO}$ in QCD and NLO EW ("default MC")

The contributions to the Standard Model prediction from the VBF, *VH*, $b\bar{b}H$ and $t\bar{t}H$ production mechanisms are determined using the particle-level predictions normalized with theoretical calculations and are collectively referred to as *XH*.

H→γγ - EFT

arXiv:1802.04146v1

- The strength and tensor structure of the Higgs-boson interactions can be investigated using an effective field theory
- additional CP-even and CP-odd interactions that change the event rates and the kinematic properties of the Higgs boson and associated jet spectra are introduced

$$\mathcal{L}_{\rm eff} = \bar{c}_g O_g + \bar{c}_{HW} O_{HW} + \bar{c}_{HB} O_{HB} + \tilde{c}_g \tilde{O}_g + \tilde{c}_{HW} \tilde{O}_{HW} + \tilde{c}_{HB} \tilde{O}_{HB},$$

c are dimensionless Wilson coefficients specifying the strength of the new CP-even and CP-odd interactions, respectively,

Oi and O˜i are dimension-six operators

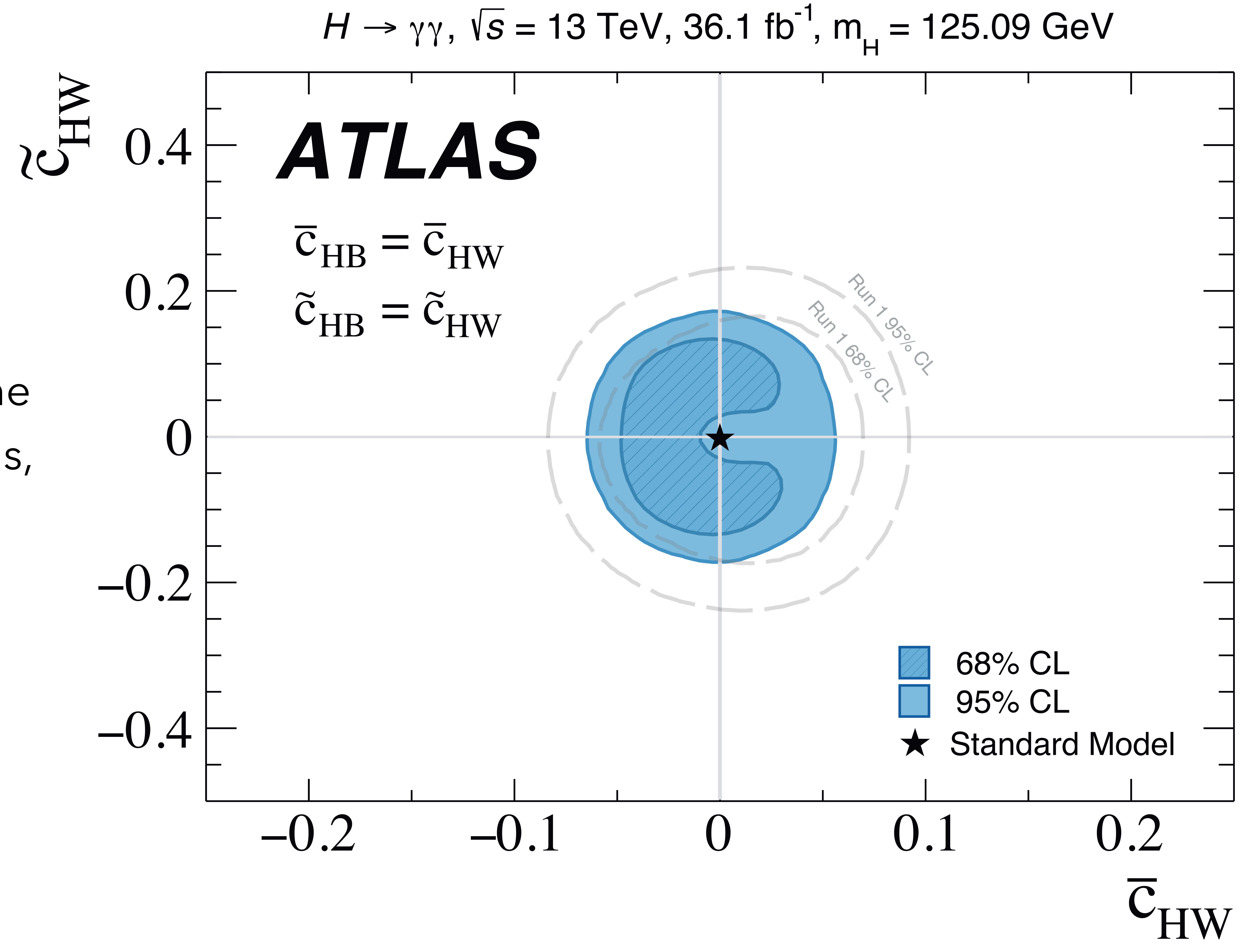

$H \rightarrow \gamma\gamma$ - Fiducial

arXiv:1802.04146v1

Fiducial region definition

Table 14: Summary of the particle-level definitions of the five fiducial integrated regions described in the text. The photon isolation $p_T^{\text{iso},0.2}$ is defined analogously to the reconstructed-level track isolation as the transverse momentum of the system of charged particles within $\Delta R < 0.2$ of the photon.

Objects	Definition
Photons	$\lvert\eta\rvert < 1.37$ or $1.52 < \lvert\eta\rvert < 2.37$, $p_T^{\text{iso},0.2}/p_T^{\gamma} < 0.05$
Jets	anti-k_t, $R = 0.4$, $p_T > 30$ GeV, $\lvert y\rvert < 4.4$
Leptons, ℓ	e or μ, $p_T > 15$ GeV, $\lvert\eta\rvert < 2.47$ for e (excluding $1.37 < \lvert\eta\rvert < 1.52$) and $\lvert\eta\rvert < 2.7$ for μ
Fiducial region	**Definition**
Diphoton fiducial	$N_\gamma \geq 2$, $p_T^{\gamma_1} > 0.35\, m_{\gamma\gamma} = 43.8$ GeV, $p_T^{\gamma_2} > 0.25\, m_{\gamma\gamma} = 31.3$ GeV
VBF-enhanced	Diphoton fiducial, $N_j \geq 2$ with $p_T^{\text{jet}} > 25$ GeV, $m_{jj} > 400$ GeV, $\lvert\Delta y_{jj}\rvert > 2.8$, $\lvert\Delta\phi_{\gamma\gamma,jj}\rvert > 2.6$
$N_{\text{lepton}} \geq 1$	Diphoton fiducial, $N_\ell \geq 1$
High E_T^{miss}	Diphoton fiducial, $E_T^{\text{miss}} > 80$ GeV, $p_T^{\gamma\gamma} > 80$ GeV
$t\bar{t}H$-enhanced	Diphoton fiducial, $(N_j \geq 4, N_{b\text{-jets}} \geq 1)$ or $(N_j \geq 3, N_{b\text{-jets}} \geq 1, N_\ell \geq 1)$

Table 16: The expected uncertainties, expressed in percent, in the cross sections measured in the diphoton fiducial, VBF-enhanced, $N_{\text{lepton}} \geq 1$, $t\bar{t}H$-enhanced, and high E_T^{miss} regions. The fit systematic uncertainty includes the effect of the photon energy scale and resolution, and the impact of the background modeling on the signal yield. The theoretical modeling uncertainty is defined as the envelope of the signal composition, the modeling of Higgs boson transverse momentum and rapidity distribution, and the uncertainty of parton shower and the underlying event (labeled as "UE/PS") as described in Section 7.4.

Source	Uncertainty in fiducial cross section				
	Diphoton	VBF-enhanced	$N_{\text{lepton}} \geq 1$	$t\bar{t}H$-enhanced	High E_T^{miss}
Fit (stat.)	17%	22%	72%	176%	53%
Fit (syst.)	6%	9%	27%	138%	13%
Photon energy scale & resolution	4.3%	3.5%	3.1%	10%	4.1%
Background modelling	4.2%	7.8%	26.7%	138%	12.2%
Photon efficiency	1.8%	1.8%	1.8%	1.8%	1.9%
Jet energy scale/resolution	-	8.9%	-	4.5%	6.9%
b-jet flavor tagging	-	-	-	3%	-
Lepton selection	-	-	0.7%	0.2%	-
Pileup	1.1%	2.9%	1.3%	2.5%	2.5%
Theoretical modeling	0.1%	4.5%	4.0%	8.1%	31%
Signal composition	0.1%	4.5%	3.1%	8.1%	25%
Higgs boson p_T^H & $\lvert y_H\rvert$	0.1%	0.9%	0.2%	0.7%	0.1%
UE/PS	-	0.3%	0.7%	1.1%	31%
Luminosity	3.2%	3.2%	3.2%	3.2%	3.2%
Total	18%	26%	77%	224%	63%

Uncertainties

HZZ STXS

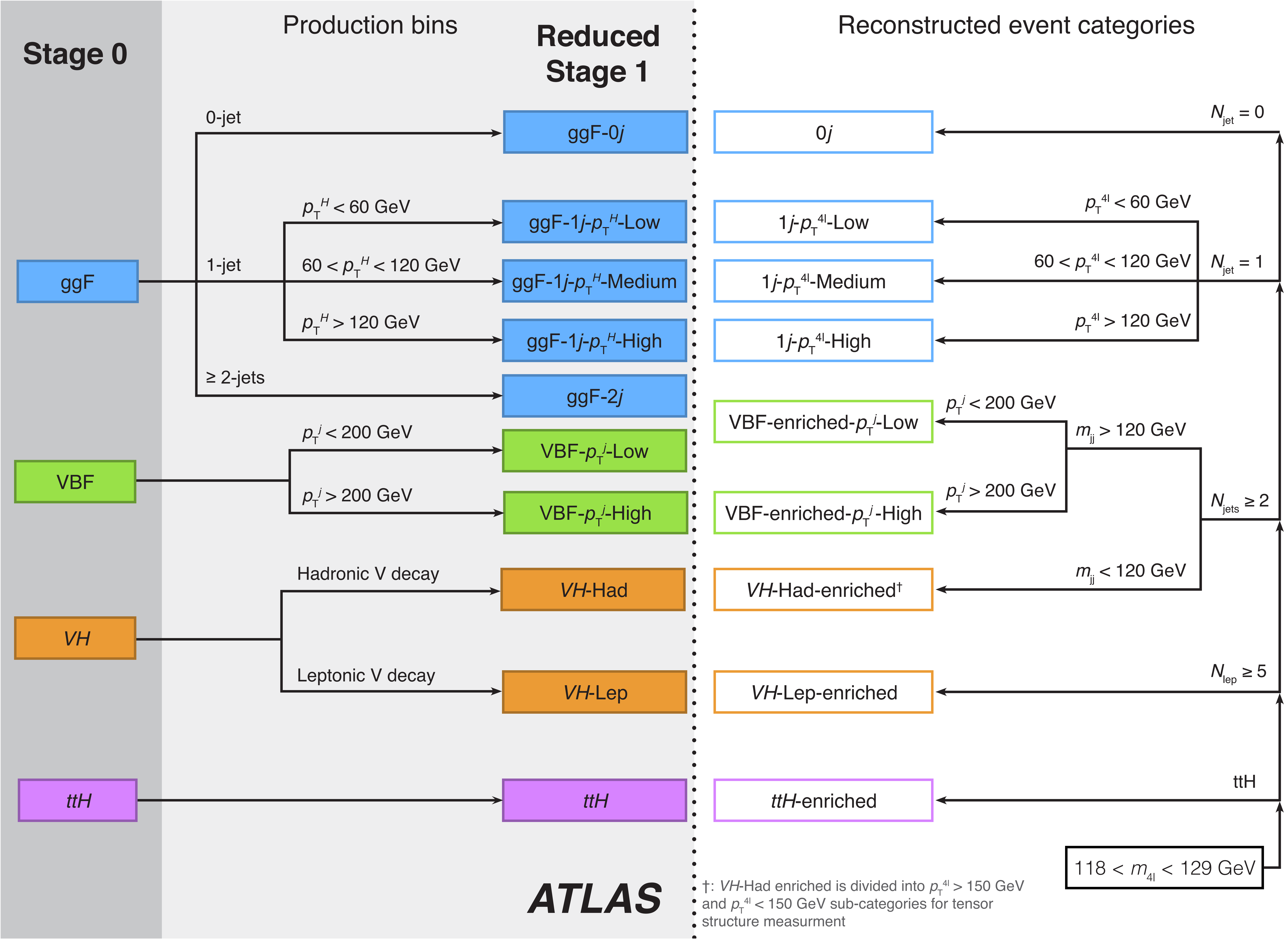

Stage 0
Production bins
Reduced Stage 1
Reconstructed event categories
ggF
VBF
VH
ttH
0-jet
1-jet
≥ 2-jets
$p_T^H < 60$ GeV
$60 < p_T^H < 120$ GeV
$p_T^H > 120$ GeV
$p_T^j < 200$ GeV
$p_T^j > 200$ GeV
Hadronic V decay
Leptonic V decay
ggF-0j
ggF-1j-p_T^H-Low
ggF-1j-p_T^H-Medium
ggF-1j-p_T^H-High
ggF-2j
VBF-p_T^j-Low
VBF-p_T^j-High
VH-Had
VH-Lep
ttH
0j
1j-p_T^{4l}-Low
1j-p_T^{4l}-Medium
1j-p_T^{4l}-High
VBF-enriched-p_T^j-Low
VBF-enriched-p_T^j-High
VH-Had-enriched†
VH-Lep-enriched
ttH-enriched
$N_{jet} = 0$
$p_T^{4l} < 60$ GeV
$60 < p_T^{4l} < 120$ GeV
$p_T^{4l} > 120$ GeV
$N_{jet} = 1$
$p_T^j < 200$ GeV
$m_{jj} > 120$ GeV
$p_T^j > 200$ GeV
$N_{jets} \geq 2$
$m_{jj} < 120$ GeV
$N_{lep} \geq 5$
ttH
$118 < m_{4l} < 129$ GeV
ATLAS
†: VH-Had enriched is divided into $p_T^{4l} > 150$ GeV and $p_T^{4l} < 150$ GeV sub-categories for tensor structure measurment

HZZ Couplings

Reconstructed event category	BDT discriminant	Input variables
$0j$	$\mathrm{BDT}_{\mathrm{ggF}}$	$p_{\mathrm{T}}^{4\ell}$, $\eta_{4\ell}$, D_{ZZ^*}
$1j$-$p_{\mathrm{T}}^{4\ell}$-Low	$\mathrm{BDT}_{\mathrm{VBF}}^{1j\text{-}p_{\mathrm{T}}^{4\ell}\text{-Low}}$	p_{T}^{j}, η_j, $\Delta R(j, 4\ell)$
$1j$-$p_{\mathrm{T}}^{4\ell}$-Med	$\mathrm{BDT}_{\mathrm{VBF}}^{1j\text{-}p_{\mathrm{T}}^{4\ell}\text{-Med}}$	p_{T}^{j}, η_j, $\Delta R(j, 4\ell)$
$1j$-$p_{\mathrm{T}}^{4\ell}$-High	-	-
VBF-enriched-p_{T}^{j}-Low	$\mathrm{BDT}_{\mathrm{VBF}}$	m_{jj}, $\Delta\eta_{jj}$, p_{T}^{j1}, p_{T}^{j2}, $\eta_{4\ell}^{*}$, $\Delta R_{jZ}^{\mathrm{min}}$, $(p_{\mathrm{T}}^{4\ell jj})_{\mathrm{constrained}}$
VBF-enriched-p_{T}^{j}-High	-	-
VH-Had-enriched	$\mathrm{BDT}_{VH\text{-Had}}$	m_{jj}, $\Delta\eta_{jj}$, p_{T}^{j1}, p_{T}^{j2}, $\eta_{4\ell}^{*}$, $\Delta R_{jZ}^{\mathrm{min}}$, η_{j1}
VH-Lep-enriched	-	-
ttH-enriched	-	-

DZZ*: difference between the logarithms of the signal and background

matrix elements squared.

Table 5: Impact of the dominant systematic uncertainties (in percent) on the measured inclusive and the Stage-0 production mode cross sections $\sigma \cdot B(H \to ZZ^*)$. Signal theory uncertainties include only acceptance effects and no uncertainty in predicted cross sections.

Production bin	Experimental uncertainties [%]: Lumi	e, μ, pile-up	Jets, flavour tagging	Higgs mass	Reducible backgr.	Theory uncertainties [%]: ZZ^* backgr.	Signal theory: PDF	QCD scale	Shower
Inclusive cross section									
	4.1	3.1	0.7	0.8	0.9	1.9	0.3	0.8	1.2
Stage-0 production bin cross sections									
ggF	4.3	3.4	1.1	1.2	1.1	1.8	0.5	1.8	1.4
VBF	2.6	2.7	10	1.3	0.9	2.2	1.6	11	5.3
VH	3.0	2.7	11	1.6	1.7	5.9	2.1	12	3.7
ttH	3.6	2.9	19	< 0.1	2.4	1.9	3.3	7.9	2.1

HZZ Fiducial and differential XS- MC

ggF ,VBF ,VH: Powheg-Box v2 Monte Carlo with PDF4LHC NLO PDF set [58].

- **ggF** is NNLO in QCD.
- The **VBF** and **VH** samples are produced at NLO accuracy in QCD. For VH, the MiNLO method is used to merge zero- and one-jet events.
- Pythia 8 is used for the H→ ZZ→4l decay as well as for parton showering, hadronization, and multiple partonic interactions.

ttH: events are simulated at NLO with MadGraph5_aMC@NLO. Herwig++ is used for parton showering and hadronization,

Alternative prediction for ggF 1: MadGraph5_aMC@NLO v.2.3.3 at NLO accuracy in QCD for zero, one, two additional jets, merged with the FxFx scheme . Interfaced to Pythia 8 for Higgs boson decay, parton showering, hadronization and multiple partonic interactions using the A14 parameter set .

Alternative prediction for ggF 2: HRes v2.3. The HRes program computes fixed-order cross sections for ggF SM Higgs boson production up to NNLO in QCD and describes the pT,4l distribution at NLO. HRes does not perform parton showering and QED final-state radiation effects are not included.

Both the MG5_aMC@NLO_FxFx and the HRes predictions are normalized using the LHCXSWG cross section (N3LO)

HZZ Event selection in fiducial phase space

Table 1: List of event selection requirements which define the fiducial phase space of the cross-section measurement. SFOS lepton pairs are same-flavour opposite-sign lepton pairs.

Leptons and jets	
Muons:	$p_{\mathrm{T}} > 5$ GeV, $\lvert\eta\rvert < 2.7$
Electrons:	$p_{\mathrm{T}} > 7$ GeV, $\lvert\eta\rvert < 2.47$
Jets:	$p_{\mathrm{T}} > 30$ GeV, $\lvert y\rvert < 4.4$
Jet–lepton overlap removal:	$\Delta R(\mathrm{jet}, \ell) > 0.1$ (0.2) for muons (electrons)
Lepton selection and pairing	
Lepton kinematics:	$p_{\mathrm{T}} > 20, 15, 10$ GeV
Leading pair (m_{12}):	SFOS lepton pair with smallest $\lvert m_Z - m_{\ell\ell}\rvert$
Subleading pair (m_{34}):	remaining SFOS lepton pair with smallest $\lvert m_Z - m_{\ell\ell}\rvert$
Event selection (at most one quadruplet per channel)	
Mass requirements:	50 GeV$< m_{12} <$ 106 GeV and 12 GeV$< m_{34} <$ 115 GeV
Lepton separation:	$\Delta R(\ell_i, \ell_j) > 0.1$ (0.2) for same- (different-)flavour leptons
J/ψ veto:	$m(\ell_i, \ell_j) > 5$ GeV for all SFOS lepton pairs
Mass window:	115 GeV$< m_{4\ell} <$ 130 GeV

HZZ Correction factor

$$\sigma_{i,\text{fid}} = \sigma_i \times A_i \times \mathcal{B} = \frac{N_{i,\text{fit}}}{\mathcal{L} \times C_i}, \quad C_i = \frac{N_{i,\text{reco}}}{N_{i,\text{part}}},$$

Ci is the bin-by-bin correction factor for detector inefficiency and resolution

bin purity: fraction of events in a bin of the reconstructed distribution that are found in the same bin at particle level.

Slightly reduced bin purity due to detector resolution effects result in larger bin migration effects, which is enhanced by the presence of a steep slope.

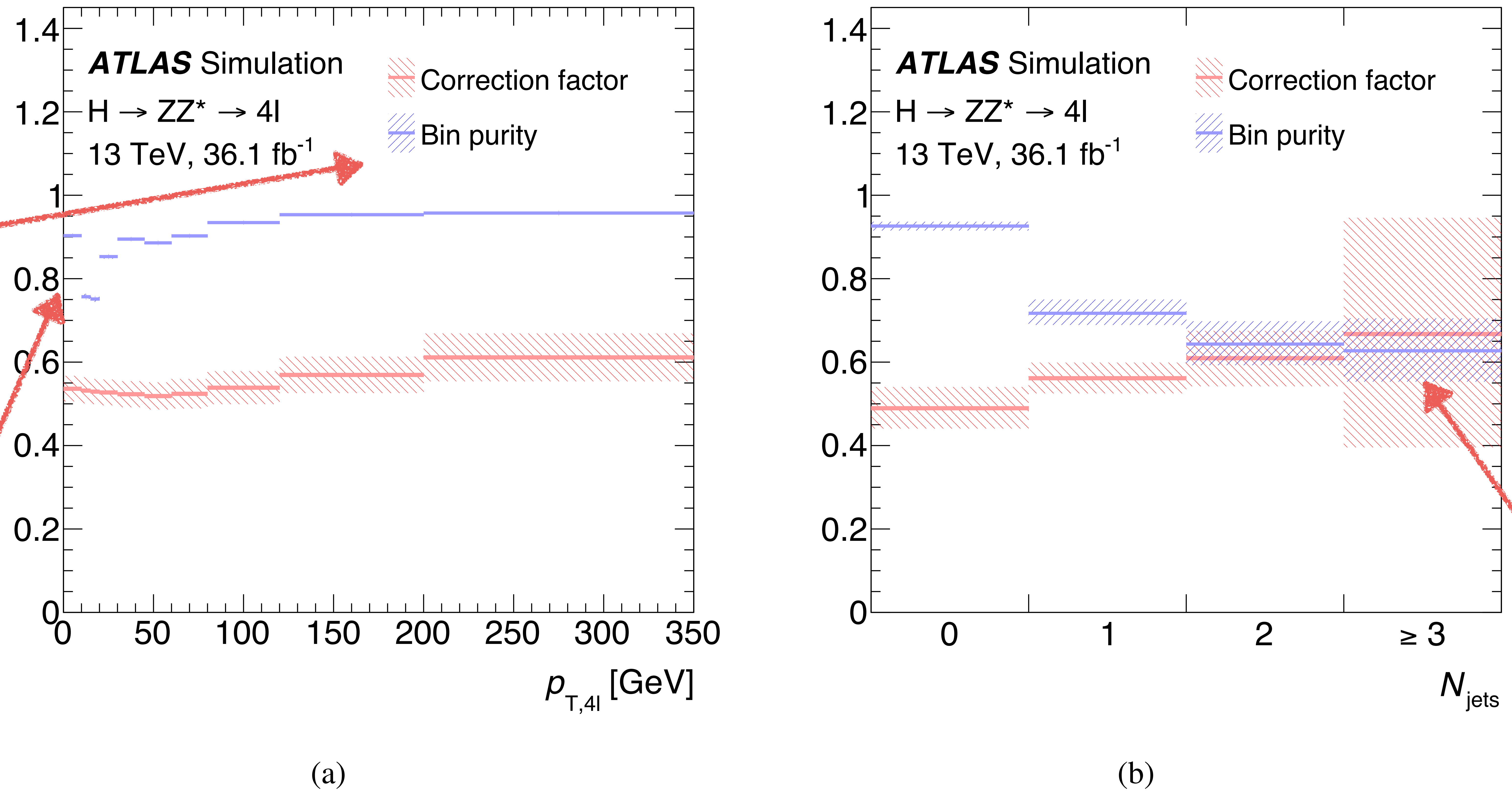

Figure 6: Bin-by-bin correction factors and bin purities for (a) the transverse momentum of the four leptons $p_{\mathrm{T},4\ell}$ and (b) the number of jets N_{jets}. The bands show the systematic uncertainties in the correction factors, which are discussed in Section 9. The uncertainties in the bin purity include the detector response and pile-up uncertainties.

Ni,reco is the number of reconstructed signal events ***Ni,part*** is the number of events at the particle level in the fiducial phase-space.

The correction factor is calculated from simulated Higgs boson samples, assuming SM production mode

The large uncertainty for *Njets* 3 is due to the experimental jet reconstruction uncertainties and the variations of the fractions of Higgs boson production modes

HZZ Fiducial and differential XS- Uncertainties

Table 3: Fractional uncertainties for the inclusive fiducial cross section σ_{comb}, obtained by combining all decay channels, and ranges of systematic uncertainties for the differential observables. The columns e, μ, jets represent the experimental uncertainties in lepton and jet reconstruction and identification. The ZZ^* theory uncertainties include the PDF and scale variations. The model uncertainties are dominated by the production mode composition variations in the extraction of the correction factors.

Observable	Stat unc. [%]	Systematic unc. [%]	Dominant systematic components [%] e	μ	jets	ZZ^* theo	Model	Z + jets+ $t\bar{t}$	Lumi
σ_{comb}	14	7	3	3	< 0.5	2	0.8	0.8	4
$d\sigma$ / $dp_{T,4\ell}$	30–150	3–11	1–4	1–3	< 0.5	< 7	< 6	1–6	3–5
$d\sigma$ / $dp_{T,4\ell}$ (0j)	31–52	10–18	2–5	1–4	3–16	3–8	1	2–3	3–5
$d\sigma$ / $dp_{T,4\ell}$ (1j)	35–15	6–30	1–4	1–3	2–29	1–4	1–11	1–2	3–5
$d\sigma$ / $dp_{T,4\ell}$ (2j)	30–41	5–21	1–3	1–3	2–19	1–5	1–7	1–2	3–5
$d\sigma$ / $d\|y_{4\ell}\|$	29–120	5–8	2–4	2–3	< 0.5	1–2	< 1	1	3–5
$d\sigma$ / $d\|\cos\theta^*\|$	31–100	5–8	2–4	2–3	< 0.5	1–2	< 2	1–4	3–5
$d\sigma$ / dm_{34}	26–53	4–13	2–5	1–5	< 0.5	1–6	< 1	1–3	3–5
$d^2\sigma$ / $dm_{12}dm_{34}$	21–40	4–12	2–4	1–4	< 0.5	1–6	< 1	1–4	3–5
$d\sigma$ / dN_{jets}	22–44	6–31	1–4	1–3	4–22	2–4	1–22	1–2	3–5
$d\sigma$ / $dp_T^{\text{lead.jet}}$	30–53	5–18	1–4	1–3	3–16	2–3	1–8	1–2	3–5
$d\sigma$ / $d\Delta\phi_{jj}$	29–43	9–17	1–3	1–3	8–14	3–4	1–7	1	3–5
$d\sigma$ / dm_{jj}	23–100	9–27	1–4	1–4	8–24	3–8	1–7	< 3	3–5

H→ZZ - EFT

In order to study the tensor structure of the Higgs boson couplings to SM gauge bosons, interactions of the Higgs boson with these SM particles are described in terms of the effective Lagrangian of the Higgs characterization model

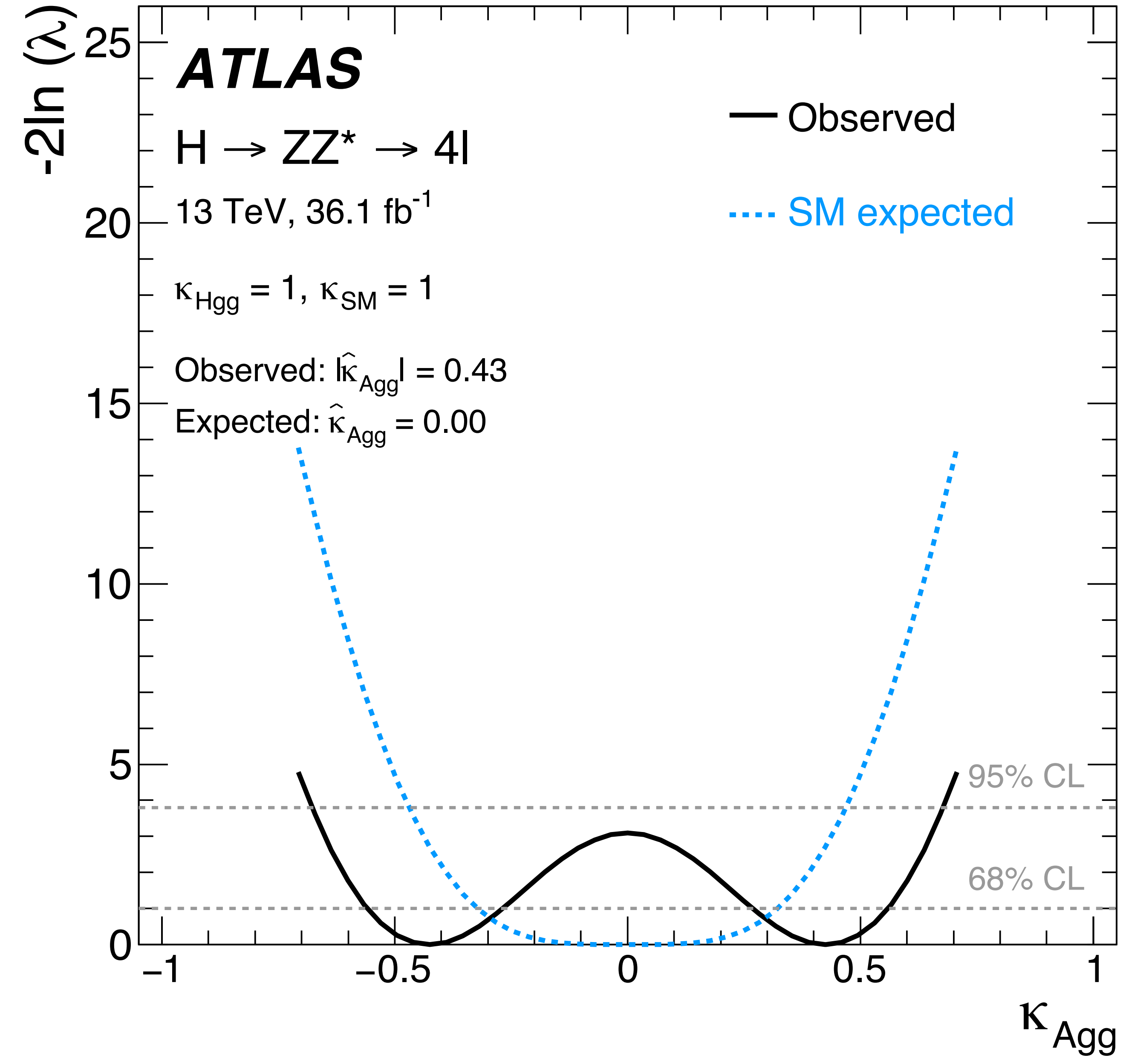

(a)

$$
\begin{aligned}
\mathcal{L}_0^V = \Bigg\{ & \kappa_{\mathrm{SM}} \left[\frac{1}{2} g_{HZZ} Z_\mu Z^\mu + g_{HWW} W_\mu^+ W^{-\mu} \right] \\
& - \frac{1}{4} \left[\kappa_{Hgg} g_{Hgg} G_{\mu\nu}^a G^{a,\mu\nu} + \tan\alpha\, \kappa_{Agg} g_{Agg} G_{\mu\nu}^a \tilde{G}^{a,\mu\nu} \right] \\
& - \frac{1}{4} \frac{1}{\Lambda} \left[\kappa_{HZZ} Z_{\mu\nu} Z^{\mu\nu} + \tan\alpha\, \kappa_{AZZ} Z_{\mu\nu} \tilde{Z}^{\mu\nu} \right] \\
& - \frac{1}{2} \frac{1}{\Lambda} \left[\kappa_{HWW} W_{\mu\nu}^+ W^{-\mu\nu} + \tan\alpha\, \kappa_{AWW} W_{\mu\nu}^+ \tilde{W}^{-\mu\nu} \right] \Bigg\} \mathcal{X}_0 .
\end{aligned}
$$

κ_{HVV} CP-even (scalar)

κ_{AVV} CP-odd (pseudo-scalar)

BSM interaction with vector bosons and the

κ_{Agg} CP-odd BSM interaction with gluons, respectively

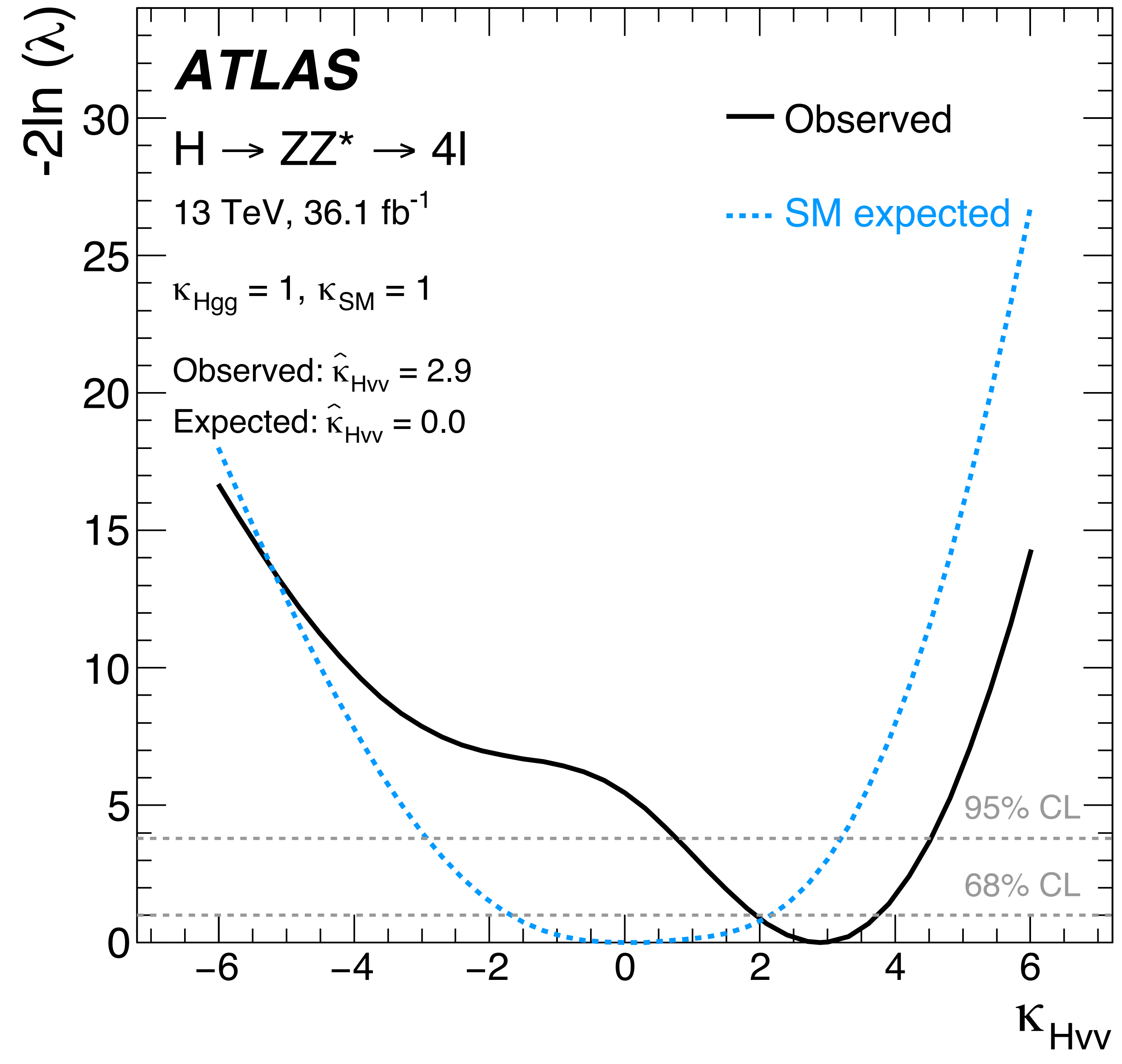

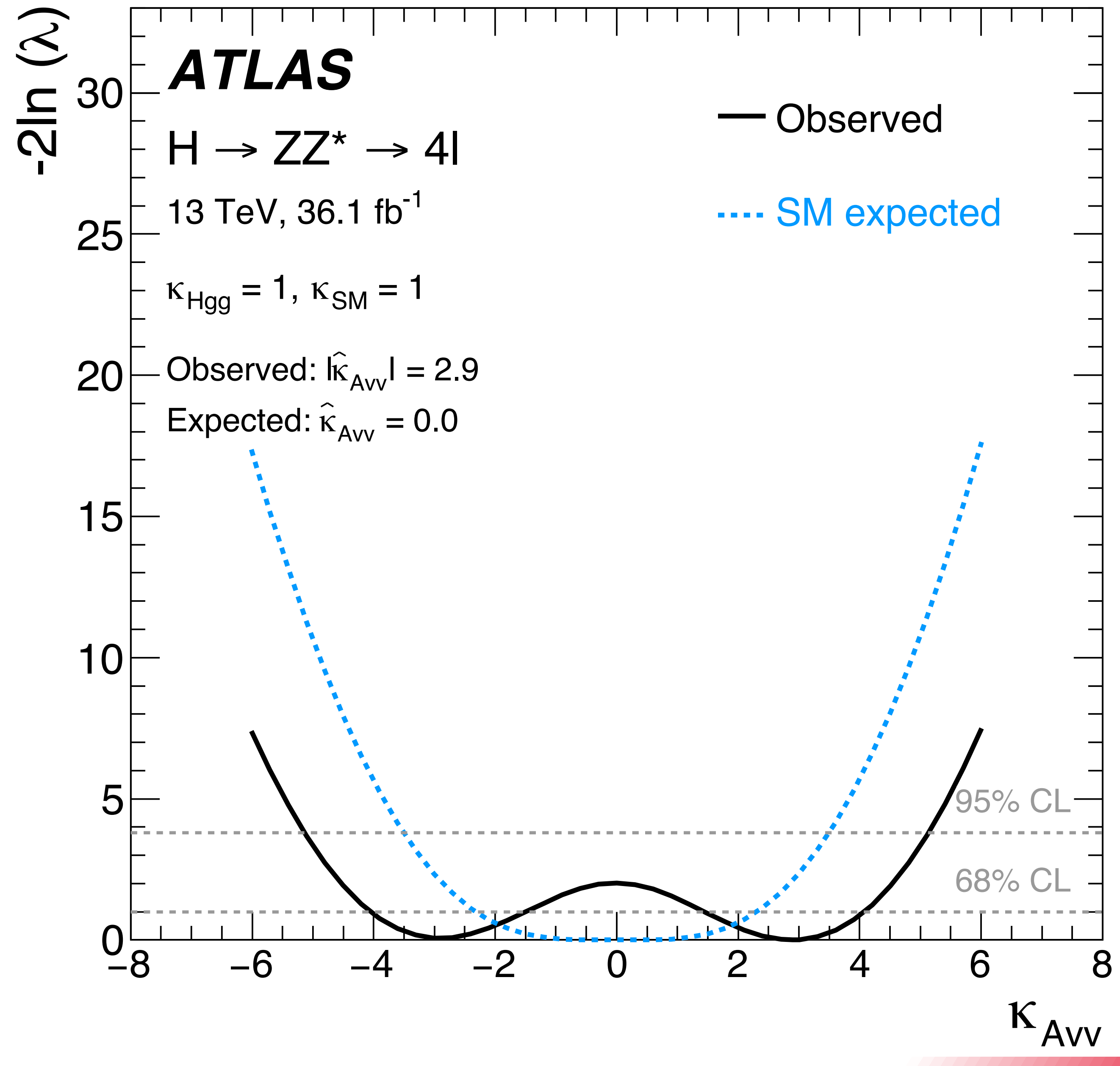

L. S. Bruni

ATLAS-CONF-2018-002

H4ℓ, Hγγ combination - differential distributions

Yields measured in the $H \to \gamma\gamma$ and $H \to ZZ* \to 4\ell$ decay channels, which are combined accounting for detector efficiencies, resolution, acceptances and branching fractions.

$$\sigma_i = \frac{N_i^{\mathrm{sig}}}{L\,\mathcal{B}\,\mathcal{A}_i\,C_i}$$

Acceptance factors :
50% $H \to \gamma\gamma$
42% $H \to ZZ* \to 4\ell$

$p_{\mathrm{T}}^{\mathrm{H}}$ Sensitive to perturbative QCD calculations

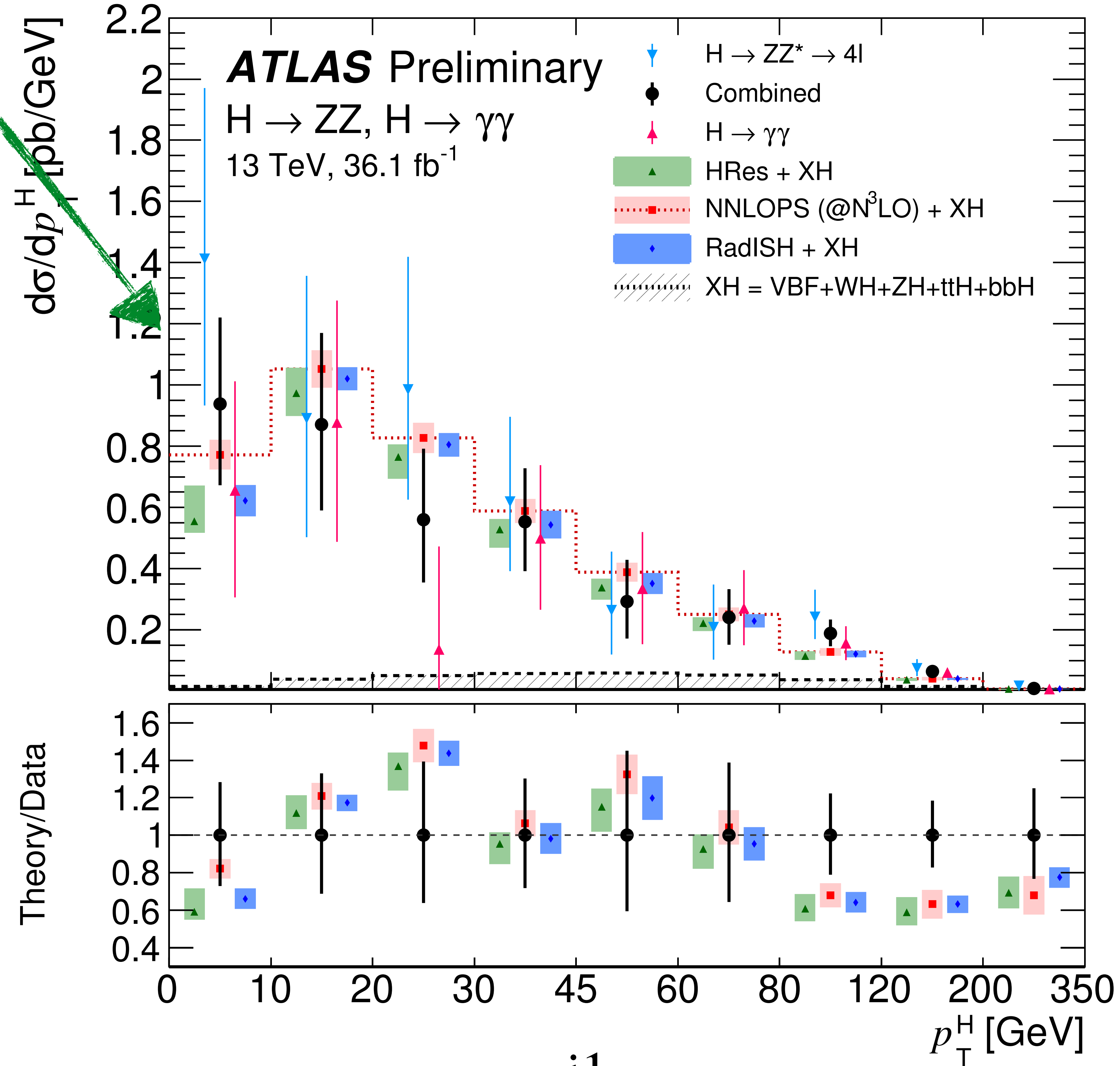

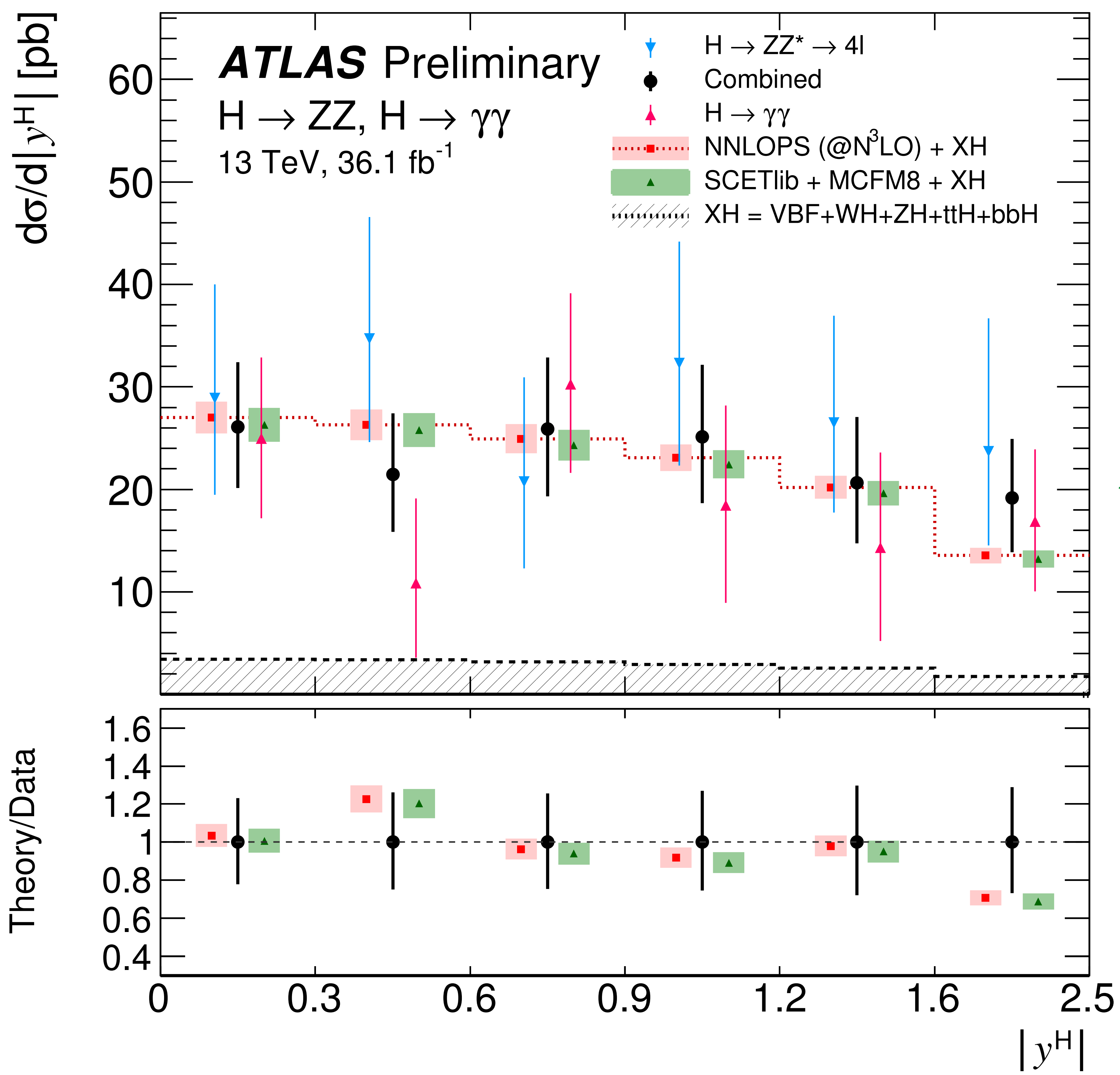

$|y^{\mathrm{H}}|$ Sensitive to the parton distribution functions

Measurements dominated by statistical uncertainties (20% - 30%)

Other: $N_{\mathrm{jets}}, p_{\mathrm{T}}^{\mathrm{j1}}$: probe the theoretical modelling of high-transverse momentum QCD radiation

H4ℓ, Hγγ combination - uncertainties

Source	Up	Down
Theoretical		
$\sigma_{\mathrm{ggF}}^{\mathrm{SM}}$ (perturbative)	−0.045	+0.044
PDFs	±0.018	
Branching fractions	±0.014	
α_S	−0.011	+0.012
Experimental		
Luminosity	−0.037	+0.038
Energy resolution (e, γ)	+0.021	−0.019
Pileup	+0.014	−0.015